university of groningen

Diagnostic Techniques in Ophthalmology

Nomdo M. Jansonius

Diagnostic Techniques in Ophthalmology

Version: November 16, 2022.
Course: Biomedical Engineering, Biomedical Instrumentation I and II

Prof. N.M. (Nomdo) Jansonius
Dept. of Ophthalmology
UMCG
University of Groningen
The Netherlands

For feedback, suggestions, and errors: n.m.jansonius@umcg.nl

Contents

Chapter 1

Visual Acuity

The assessment of the visual acuity (VA) is by far the most commonly performed test in ophthalmology. It aims to measure the spatial resolution of the eye - or better - the visual system. A normal VA requires intact optics (clear cornea and lens, and glasses if needed), a normal function of the central retina (fovea) and optic nerve, and intact visual pathways beyond the optic nerve (chiasm, optic tract, thalamus, optic radiation, and visual cortex).

Herman Snellen, a Dutch ophthalmologist, is considered the inventor of this test. Figure 1.1 (left panel) shows the design of the original VA chart from the middle of the 19th century.

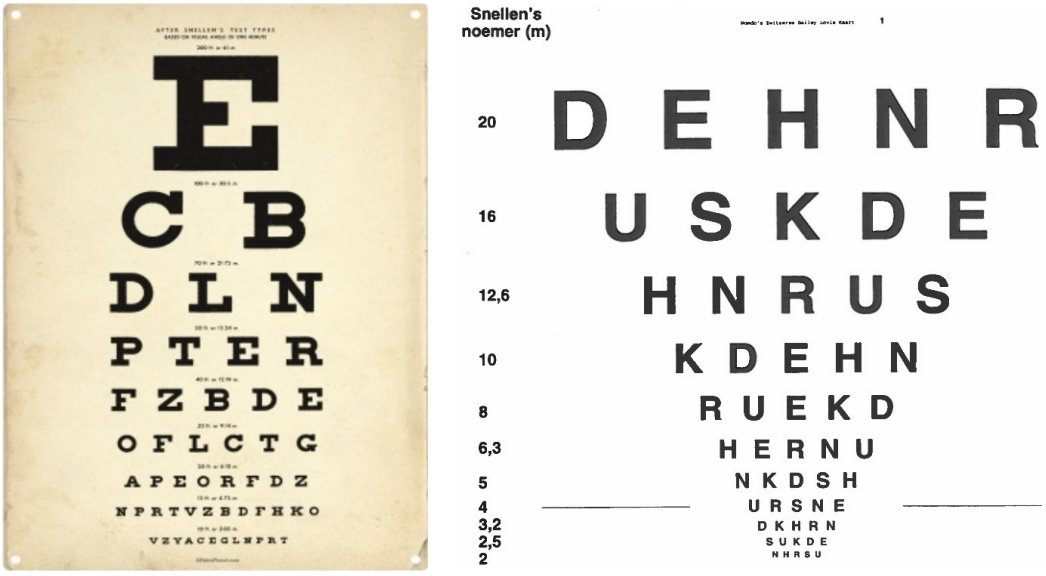

Figure 1.1: Original design of the Snellen visual acuity chart (left) and of a modern visual acuity chart (right).

The original chart had several limitations. For example, the number of 'optotypes' and their spacing varied between the lines, the relative change in optotype size between the lines decreased from top to bottom, and the legibility varied between the optotypes.

1.1 Visual acuity chart: layout and usage

Figure 1.1 (right panel) presents a modern VA chart. It contains 5 optotypes per row ('line'). The spacing between the lines equals the size of the optotypes below the spacing. The size changes between the lines with a factor of 1.26, that is, 0.1 log units. This implies 0.3 log units with three lines, that is, a doubling or halving of the size ($1.26^3 = 2$, $1.26^{-3} = 0.5$). Next to each line a number is given: the denominator of Snellen, or D. This number reflects the average distance at which a healthy eye is just able to resolve the corresponding optotypes.

A VA chart is mounted at a wall and well illuminated. A subject reads the optotypes from a distance d. The D value of the last line with at least 3 of 5 optotypes recognized correctly is recorded and used to calculate the VA:

$$\text{VA} = d/D \tag{1.1}$$

Hence, following Eq. (1.1), a normal VA is, by definition, 1.0, and if someone is able to read at $d = 6$ m optotypes with size $D = 12$ m, the VA is 0.5. Young, healthy subjects often have a VA above 1.0, being 1.25, 1.6, or even 2.0. Above 50 years of age, 0.8 is considered normal as well.

1.2 Optotype size and minimal angle of resolution

Optotypes are designed on a 5x5 grid (Figure 1.2). A VA of 1.0 corresponds to an optotype height of 5 arcmin and a gap size of 1 arcmin (Figure 1.2), that is, the typical spatial resolution (according to the Raleigh criterion) of the visual system is 1 arcmin. The gap size is also called the minimal angle of resolution (MAR), and an alternative way for expressing visual acuity is the logMAR, where the base of the logarithm is 10 and MAR in arcmin.

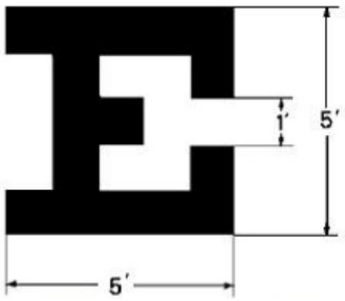

Figure 1.2: Gap and optotype size at a visual acuity of 1.0.

Clinicians prefer decimal notation; logMAR is the preferred format is scientific articles. Decimal and logMAR VA can easily be transformed into each other:

$$\text{VA(logMAR)} = \log(1/\text{VA(decimal)}) = -\log(\text{VA(decimal)}) \tag{1.2}$$

Table 1.1 illustrates how the various VA metrics relate to each other.

Table 1.1: Relationship between visual acuity in Snellen notation, decimal notation, and logMAR, for $d = 6$ m

D (m)	VA (Snellen)	VA (decimal)	VA (logMAR)
30	6/30	0.2	0.7
24	6/24	0.25	0.6
19		0.32	
15		0.4	
12	6/12	0.5	0.3
9.5		0.64	
7.5		0.8	
6	6/6	1.0	0.0
4.8		1.25	
3.8		1.6	
3	6/3	2.0	-0.3

1.3 Influence of eccentricity and luminance

Spatial resolution is always measured at high contrast: a VA chart has black optotypes on a white background. The ability of the visual system to detect low contrasts (small luminance differences) can be assessed with a contrast sensitivity test (Chapter 2). Visual acuity is measured foveally (at fixation); it declines rapidly towards the periphery of the retina. Figure 1.3 (left panel) shows VA as a function of eccentricity (distance from fixation). In clinical practice, however, the function of the peripheral retina is not tested with a VA test at different eccentricities, but with a technique called perimetry (Chapter 3).

Figure 1.3 (right panel) shows the influence of luminance on VA. The discontinuity (in the first derivative) at approximately -0.5 photons corresponds to the transition from scotopic to photopic vision. Scotopic vision refers to vision with rods; photopic vision to vision with cones. To ensure being in the saturated part of the curve, a luminance of the VA chart of at least 100 cd/m^2 should be used.

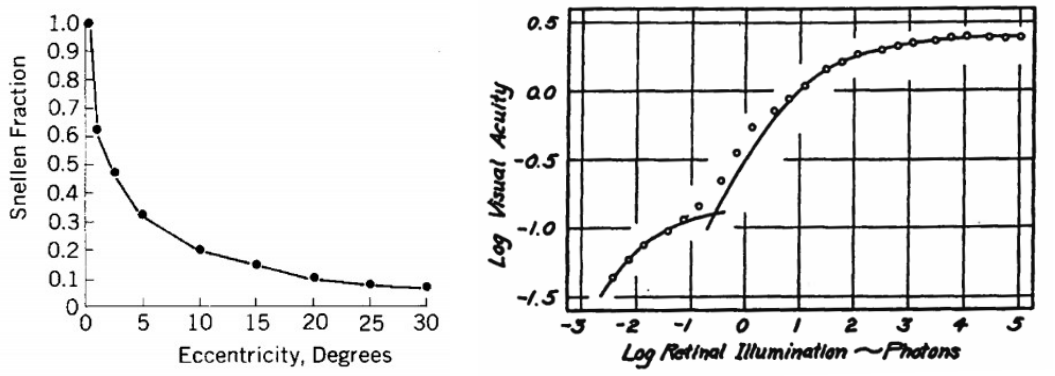

Figure 1.3: Visual acuity as a function of eccentricity (left; [19]) and luminance (right; [17]). Note: the historical quantity and unit 'retinal illumination' and 'photons' were later replaced by 'retinal illuminance' and 'troland' (Td), respectively. At the recommended minimum luminance of a visual acuity chart of 100 cd/m^2, the pupil diameter of the human eye is approximately 2.5 mm [18]. Hence, a luminance of 100 cd/m^2 yields a retinal illuminance of approximately 500 Td (see Chapter 4 for explanation), which is between 2 and 3 photons (100 and 1000 Td), close to where the curve starts to saturate.

Exercises

1. A VA chart is mounted on a wall 4 m in front of a subject. Next to the last line read correctly by the subject, a number is printed on the chart: 12. What does this number mean? Calculate the VA of the subject (in decimal notation).

2. The same chart is moved to 6 m in front of the same subject. What is now the VA? And which number will now be next to the last line read correctly?

3. Calculate the visual acuity in logMAR of the subject of Exercises 1 and 2.

4. Complete Table 1.1.

5. What is the height (size), in mm, of an optotype corresponding to a VA of 1.0 if measured at a distance of 6 m (that is, $D = 6$ m)?

6. Newspaper print has a typical letter height of 2 mm. What is the corresponding D (denominator of Snellen)? Can you read a newspaper at that distance?

7. A computer screen measures 30x23 cm and has a resolution of 1024x768 pixels. The viewing distance is 60 cm. What is the angular distance between the pixels? Conclusion?

Chapter 2

Contrast sensitivity

Contrast sensitivity (CS) refers to the smallest luminance *difference* a visual system is able to detect. Unlike visual acuity (VA) testing, contrast sensitivity testing is not done routinely in all patients. However, it plays a major role in clinical science.

2.1 Contrast and contrast sensitivity

An easy way to assess the contrast sensitivity is with the Pelli-Robson test: a wall chart with optotypes, all with the same size but with decreasing contrast (Figure 2.1).

Figure 2.1: Pelli-Robson contrast sensitivity test.

The contrast of an optotype is expressed as Weber contrast:

$$\text{Contrast} = \frac{L_o - L_b}{L_b} \tag{2.1}$$

where L_o is the luminance of the optotype and L_b the luminance of the background. Contrast

sensitivity is the (absolute value of) the reciprocal of the smallest contrast (threshold contrast) someone is able to detect:

$$\text{CS} = \frac{1}{|\text{threshold contrast}|} \tag{2.2}$$

It is usually reported as the logarithm to base 10 of CS: logCS. On the Pelli-Robson chart, the logCS increases with 0.15 per triplet (group of three optotypes with the same contrast); the last triplet with at least 2 of 3 optotypes recognized correctly corresponds to the logCS. The chart is read at a distance of 1 or 3 m with optimal correction (with glasses) for the viewing distance. This is important: CS halves per diopter of optical blur. Similarly, the luminance must be sufficiently high - the recommended range is between 60 and 120 cd/m^2 (for definition of luminance see Chapter 4).

A more thorough assessment of the CS is the measurement of the contrast sensitivity for a series of sinusoidal gratings ranging from low to high spatial frequency (Figure 2.2).

Figure 2.2: Sinusoidally modulated gratings, from low to high spatial frequency.

For a grating, the contrast is expressed as Michelson contrast:

$$\text{Contrast} = \frac{L_{max} - L_{min}}{L_{max} + L_{min}} \tag{2.3}$$

where L_{max} and L_{min} are the maximum and minimum luminance within the grating, respectively. Again, CS is the reciprocal of threshold contrast.

2.2 Contrast sensitivity function

CS or logCS plotted as a function of spatial frequency is called the contrast sensitivity function (CSF; Figure 2.3).

One of the most striking aspects of the CSF is the decrease in logCS at low spatial frequencies. This decline is related to lateral inhibition, an important aspect of the (pre)processing of visual information in the retina. Lateral inhibition originates in the horizontal cells in the retina and causes the characteristic center-surround receptive field sensitivity profile of the retinal ganglion cells. These cells respond strongly to small stimuli in the center of their receptive field but

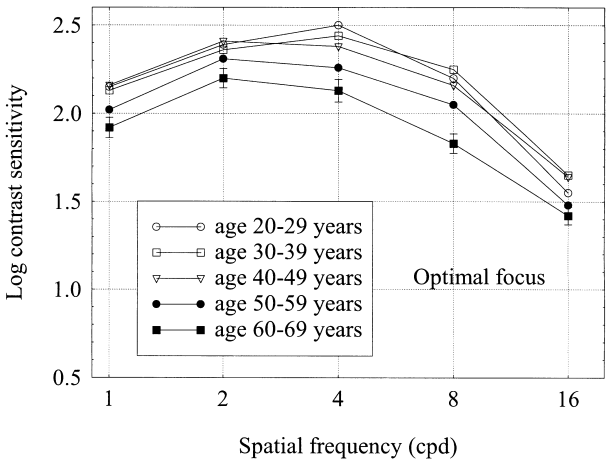

Figure 2.3: Contrast sensitivity function (CSF) for different age categories [13].

hardly to diffuse illumination: in the latter case the response from the center is annihilated by an opposite response from the surround. For gratings with a spatial frequency around 3 cpd (cycles per degree of visual space), the light (or dark) bar stimulates the center and the dark (or light) bar the surround, resulting in an optimal response: the peak of the CSF occurs at about 3 cpd (Figure 2.3). More intuitively, the CSF also decreases at high spatial frequencies. For the CSF of the human eye, the highest spatial frequency that can be observed if offered at the highest possible contrast (1.0) is approximately 30 cpd. At 30 cpd, the light and dark bars have a width of 1 arcmin each, identical to the gap size of optotypes corresponding to a VA of 1.0 (Chapter 1).

2.3 Psychophysical methods for determining a threshold

Sensory cells and neural circuitries are intrinsically noisy and thus small signals (stimuli) may not be detected. If a signal is large compared to the noise, it will be detected virtually always (supra-threshold stimulus); if a signal is small compared to the noise, it will not be detected (sub-threshold stimulus). At threshold, signal and noise are of similar size, and the stimulus may or may not be detected. Usually, threshold is defined as the stimulus strength at which the stimulus is detected in 50% of the cases.

Several psychophysical methods exist that can be used to determine threshold contrast when using sinusoidal gratings. In case of the two-alternative forced choice (2AFC) method, two stimuli are presented: one with a grating and one without. The subject is asked which stimulus contains the grating and is forced to make a choice. Alternatively, a single stimulus with two different appearances may be used (for example, a grating tilted either to the left or to the right, with the subject being forced to choose between left/right tilt). The higher the contrast, the more likely it is that the correct answer is given. A third approach is the use of a single stimulus that may or may not contain a grating. However, unlike the forced choice methods,

such a yes/no approach does not result in an unbiased threshold estimate.

With 2AFC, the probability that the correct answer is given increases from 50% (random guess) for contrasts amply below threshold contrast to 100% for contrasts amply above threshold contrast. A graph showing the probability that the correct answer is given as a function of stimulus strength (contrast in case of a contrast sensitivity test) is called a psychometric function or frequency-of-seeing (FOS) curve (Figure 2.4). A probability of 75% indicates threshold contrast (50% correct above chance level). Determining a complete psychometric function may be very time-consuming. Clever algorithms (with fancy names like PEST, Best-PEST, QUEST, and ZEST) may shorten the total test time considerably.

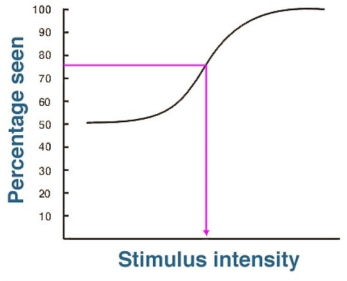

Figure 2.4: Psychometric function in 2AFC.

In clinical settings, it is not always needed to characterize the full psychometric function - it is often sufficient to estimate the threshold. This may be done simply by increasing stimulus strength until seen followed by decreasing the strength until not seen. If the change in stimulus strength is stepwise, this approach is called the staircase procedure - it is the default method used in clinical perimetry and will be further explained in the concerning chapter (Chapter 3). If the strength varies continuously, it is called von Békésy tracking.

2.4 Modulation transfer function and line spread function

The optical equivalent of the CSF is the modulation transfer function (MTF), which gives the contrast in the image of an object that is projected by an optical system divided by the contrast in the object, as a function of spatial frequency (Figure 2.5; left panel). An MTF goes from 1 at low spatial frequencies (no loss of contrast for course patterns) to 0 for spatial frequencies above the spatial resolution of the system. The image on the retina of a point source at infinity is called the point spread function (PSF). Likewise, the image of a thin line is called the line spread function (LSF). Mathematically, the Fourier transform of the MTF is the LSF (Figure 2.5; right panel). The MTF is sensitive to optical blur. For the human eye, the modulation transfer halves per diopter of optical blur for spatial frequencies above approximately 2 cpd. Below 1 cpd, on the other hand, the effect of blur becomes negligible.

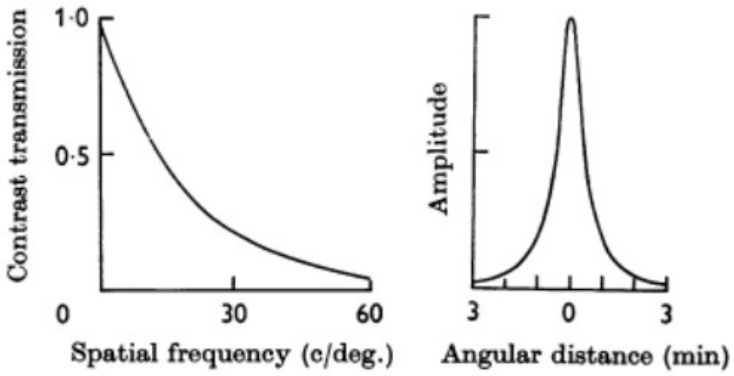

Figure 2.5: Modulation transfer function (MTF; left) and line spread function (LSF; right) of the human eye [2].

Exercises

1. The smallest contrast seen by a subject viewing a sinusoidal grating on a screen is 0.01 (1%). What is the corresponding logCS? What is the highest contrast that can be displayed for a sinusoidal grating? If this contrast value corresponds to threshold contrast for a patient, what is his/her logCS?

2. A subject reads a Pelli-Robson chart and recognizes the optotypes correctly until he makes two mistakes in the logCS = 2.05 triplet. What is the logCS of this subject? What is the corresponding contrast of the optotypes? Is this Michelson or Weber contrast?

3. The logCS of a subject as measured with adequate optical correction for the viewing distance (3 m) with the Pelli-Robson chart is 2.20. A +1 D lens is added, causing optical blur. What logCS value do you expect now? And with +2 D?

4. The optotype height of a Pelli-Robson chart is 50 mm. What is the corresponding denominator of Snellen (see Chapter 1)? The typical gap size of an optotype is 1/5 of its height (Figure 1.2); for the Pelli-Robson chart this gap size is 10 mm. What is the gap size in armin if the chart is observed at a distance of 3 m?

5. Sketch a psychometric function for a three-alternative forced choice test (3AFC; three stimuli are presented: one with a grating and two without). What percentage along the y-axis corresponds to threshold contrast?

6. Most video cards/computer monitor combinations are 8 bit, that is, the system can display 256 gray levels. Assume a background luminance of 50% of maximum luminance. What is the smallest a) Weber contrast and b) Michelson contrast this system can display? You may assume a linear relationship between presumed gray level and actual luminance. Is this system usable to build a CS testing system? Why (not)?

Chapter 3

Perimetry

Perimetry refers to the assessment of the visual field; the visual field loosely represents vision outside the fovea. Figure 3.1 presents a cartoon depicting the essence of perimetry: a stimulus is provided at several locations and has to be reported as seen or not seen.

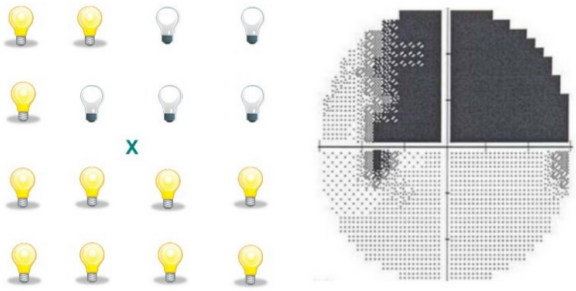

Figure 3.1: Essence of perimetry. x = fixation point.

In clinical practice, perimetry is especially important for the detection and monitoring of diseases that (in an early stage) do not affect visual acuity, like glaucoma (left panel of Figure 3.2). Glaucoma is a neurodegenerative disease of the retinal ganglion cells and optic nerve. Perimetry can also be used for the detection of brain lesions and may give hints regarding the location of these lesions (right panel of Figure 3.2).

3.1 Standard automated perimetry

Modern perimeters use small light stimuli generated on a computer screen or projected in a bowl (if a screen is used, perimetry is formally called campimetry). In standard automated perimetry (SAP), the stimulus size (diameter) is 0.43° (26 arcmin) and the stimulus duration 200 ms. The visual field is sampled using a 6x6° grid, up to an eccentricity of typically 30°. The stimuli are projected on a background luminance of 10 cd/m^2.

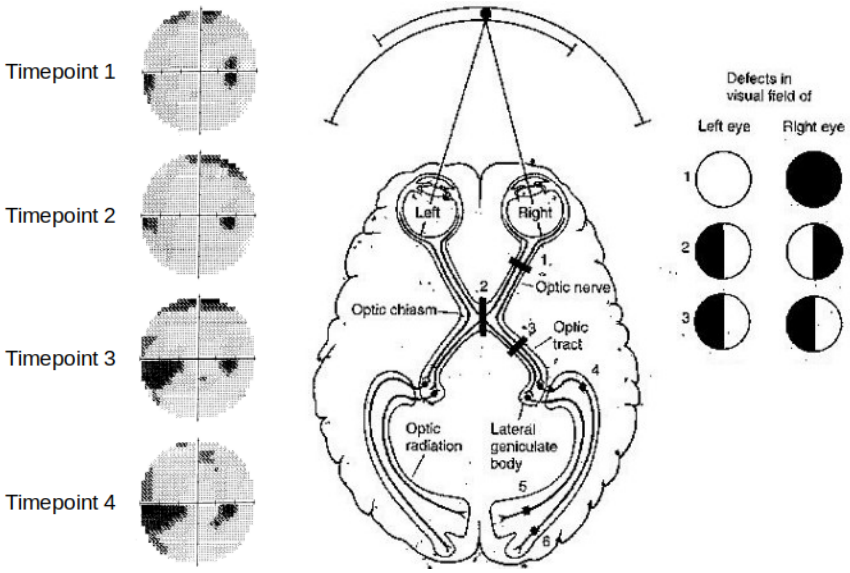

Figure 3.2: Left: Monitoring the visual field of a glaucoma patient (right eye); the visual field defect seems to increase with time. Right: Visual field abnormalities as a function of the site of a visual pathway lesion.

SAP measures the smallest difference between stimulus and background luminance a subject can detect - for each test location. This difference is called differential light sensitivity (DLS) and after normalizing to background luminance, it is threshold contrast. Weirdly, this threshold contrast is expressed in dB; 0 dB corresponds to the strongest stimulus available (which differs between different perimeter brands!) and a +3 dB step means halving of the contrast. If the healthy population has on average a threshold contrast of 30 dB in a certain test location using a certain perimeter, a value of 20 dB in a patient (a -10 dB step, that is, a factor 10 increase in threshold contrast) means a loss of 90% of the sensitivity in the concerning test location.

The psychophysical method underlying SAP is a so called staircase procedure. The intensity increases in 4 dB steps until seen and subsequently decreases in 2 dB steps until not seen; the threshold is halfway the last seen and the final not seen. This is repeated for all test locations. Clever algorithms estimate the initial value of the staircase from population data and results from neighboring test locations, and in this way the testing time is shortened considerably.

Figure 3.3 shows the printout of a commonly used perimeter, the Humphrey Field Analyzer (HFA). This printout shows a normal visual field. The most important metric to summarize the visual field is the 'mean deviation' (MD). The MD is the mean loss in dB, averaged over all test locations - with age-similar healthy subjects as the reference. Hence, a healthy eye has an MD of 0 dB. The MD of a blind eye depends on the perimeter used (because, in perimetry, blind means "not able to see the strongest stimulus available in any test location"). For the HFA, the MD of a blind eye is approximately -30 dB.

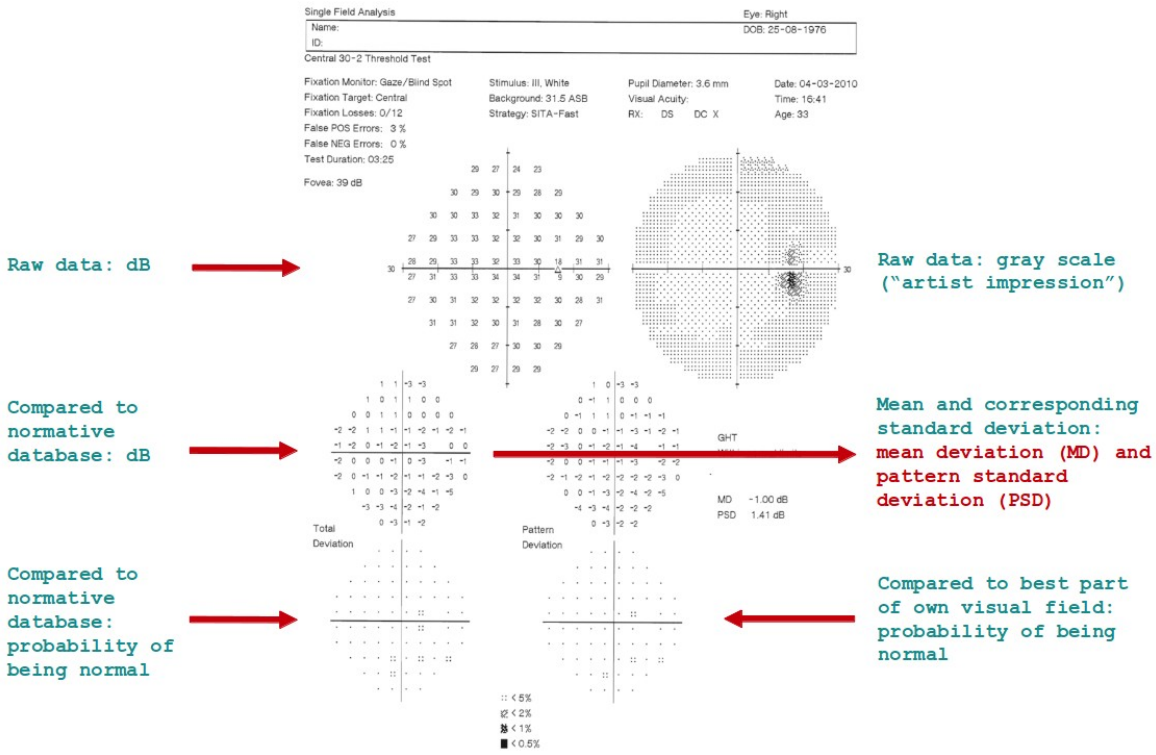

Figure 3.3: Printout of a standard automated perimetry test result with explanation of the analysis performed by the built-in software (Humphrey Field Analyzer).

Exercises

1. Which hemisphere is used to observe objects that are on the right (temporal) side of the fixation point of the right eye? And which hemisphere for objects that are on the right (nasal) side of the fixation point of the left eye?

2. Figure 3.3 shows a normal visual field. What is the origin of the scotoma (visual field defect) located at an eccentricity of approximately 15° just below the horizontal meridian? Is this a left eye or a right eye visual field? Which test location reflects the fovea?

3. Compared to a 24 dB stimulus, give for the following stimuli (1) if they are weaker or stronger and (2) by what factor: 34 dB, 29 dB, 21 dB, 18 dB, and 4 dB.

4. At the background luminance as used in perimetry, the integration time of the visual system is around 100 ms. For stimuli shorter than the integration time, the visual system cannot disentangle intensity and duration: a subject sees a short flash of which the perceived strength is determined by intensity × duration (or, more formally, the area under the intensity versus time curve). For stimuli longer than the integration time, the visual sysem can judge intensity and duration separately. A subject compares a 24 dB 100 ms stimulus (reference stimulus) to a series of stimuli. All stimuli are visible, that is, they are supra-threshold. Describe the observed

relative (that is, compared to the reference stimulus) intensity and duration for each of the following four stimuli (A-D):

A. 24 dB 50 ms

B. 24 dB 200 ms

C. 21 dB 50 ms

D. 21 dB 200 ms

5. Cataract makes the human lens acting as a blurry neutral density filter. Figure 3.4 shows the visual fields of two patients: one with cataract and one with glaucoma. Which visual field belongs tot cataract and why?

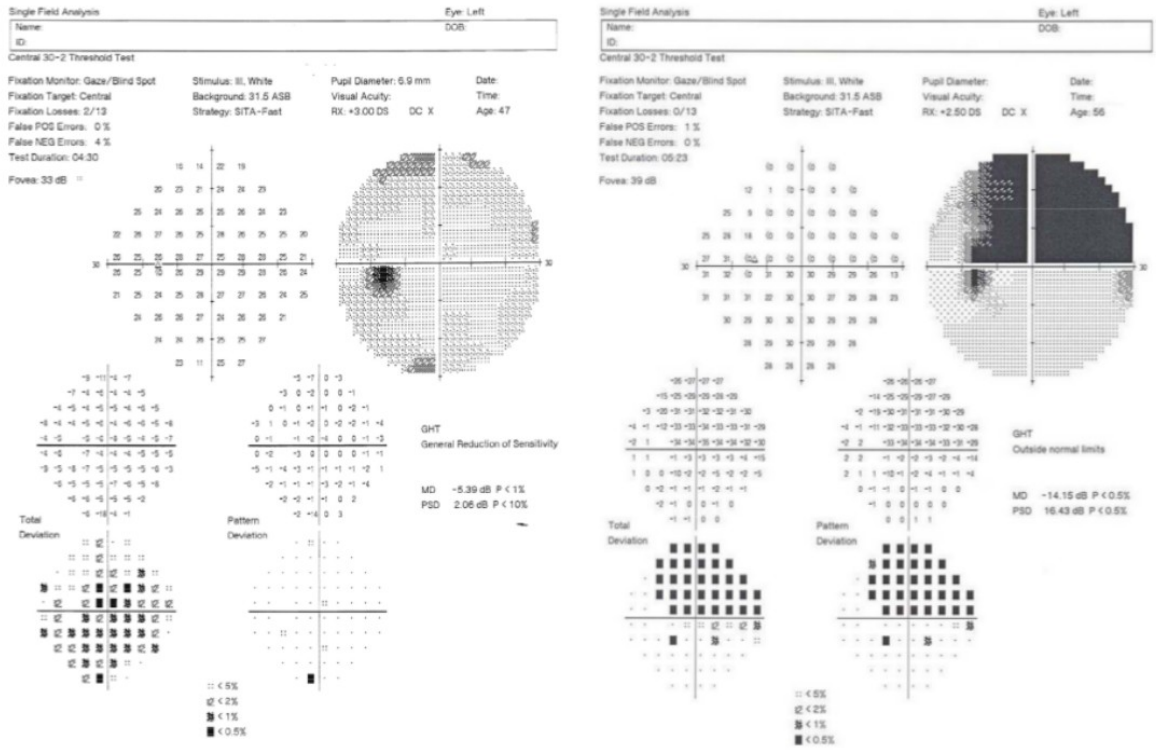

Figure 3.4: Examples of abnormal visual fields.

6. A campimeter uses a computer screen with a horizontal-to-vertical size ratio of 4:3. A subject observes the screen from a distance that equals the diagonal size of the screen. The subject fixates at the middle of the screen. What is the maximum eccentricity (distance from fixation point, measured in degrees) that can be reached horizontally? And vertically? What is the advantage of perimetry over campimetry?

7. The Humphrey Field Analyzer (HFA) has a background luminance of 10 cd/m^2 and a maximum stimulus strength projected on this background of 3162 cd/m^2. A subject has, in a certain test location, a Weber logCS of 1.0 (see Chapter 2). What is the corresponding threshold contrast in dB for this specific perimeter? And for a logCS of 0.7? 0.4?

Chapter 4

Photometry and radiometry

Radiometry refers to the measurement of the amount of electro-magnetic (EM) radiation. Photometry refers to the measurement of the amount of light, i.e., visible EM radiation. A photometer is a radiometer with a photometric filter. The transmittance of a photometric filter has been standardized in 1931 by the CIE (Commission Internationale de l'éclairage or International Commission on Illumination) and is described by the V_λ curve (Figure 4.1, left panel). Mathematically, the amount of light is the amount of EM radiation weighed to V_λ. The V_λ curve mimics the spectral sensitivity of the eye (Figure 4.1, right panel). Different curves exist for photopic vision (cone vision) and scotopic vision (rod vision), the V_λ and V'_λ curve, respectively.

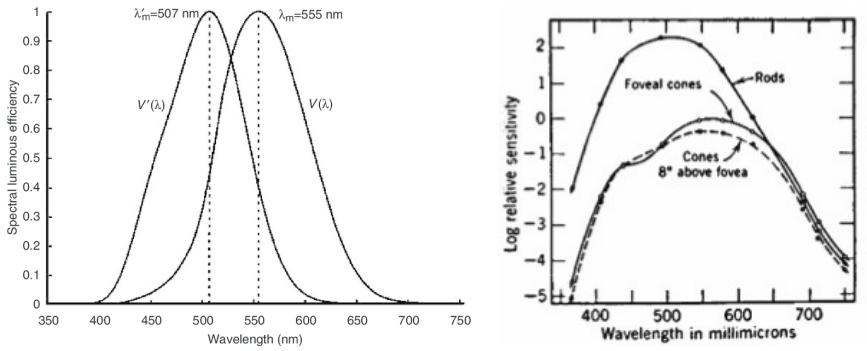

Figure 4.1: Left: V_λ and V'_λ curves (CIE 1931) [7]. Right: Spectral sensitivity of the human eye [14].

The spectral sensitivity of the eye is determined by the transmittance of the ocular media (Figure 4.2, left panel; cornea, aqueous, lens, and vitreous) and the absorptance spectra of the visual pigments in the cones and rods. Figure 4.2 (right panel) shows the absorptance spectra of the three cone types. Some formal definitions:

Transmittance: fraction of incident EM power transmitted through a sample
Reflectance: fraction of incident EM power reflected at an interface
Absorptance: fraction of incident EM power absorbed at an interface

These quantities plotted as a function of wavelength are called transmittance spectrum, reflectance spectrum, and absorptance spectrum, respectively.

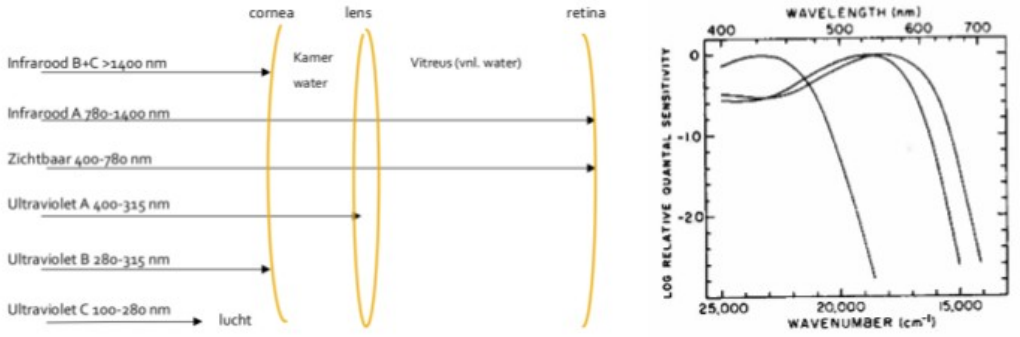

Figure 4.2: Left: Transmittance of ocular media. Right: Absorptance spectra of cone visual pigments [14].

4.1 Photometric quantities and units

The quantity used to express the amount of light provided by a light source ('visible power') is called luminous flux (S); the corresponding unit is the lumen (lm). Visual power per solid angle is called luminous intensity (I); the corresponding unit is lm/sr or candela (cd). Visible power per unit area is called illuminance (E); the corresponding unit is lm/m^2 or lux. Finally, the quantity used to express the amount of light emitted by a surface (e.g., a computer monitor) is called luminance (L); the corresponding unit is cd/m^2 (which equals lm/sr/m^2). The luminance of a surface does not depend on the viewing distance. In case of a perfectly diffusely reflecting surface (Lambertian reflectance), L and E are connected via Lambert's cosine law: $L = E/\pi$. Figure 4.3 summarizes the photometric quantities and units.

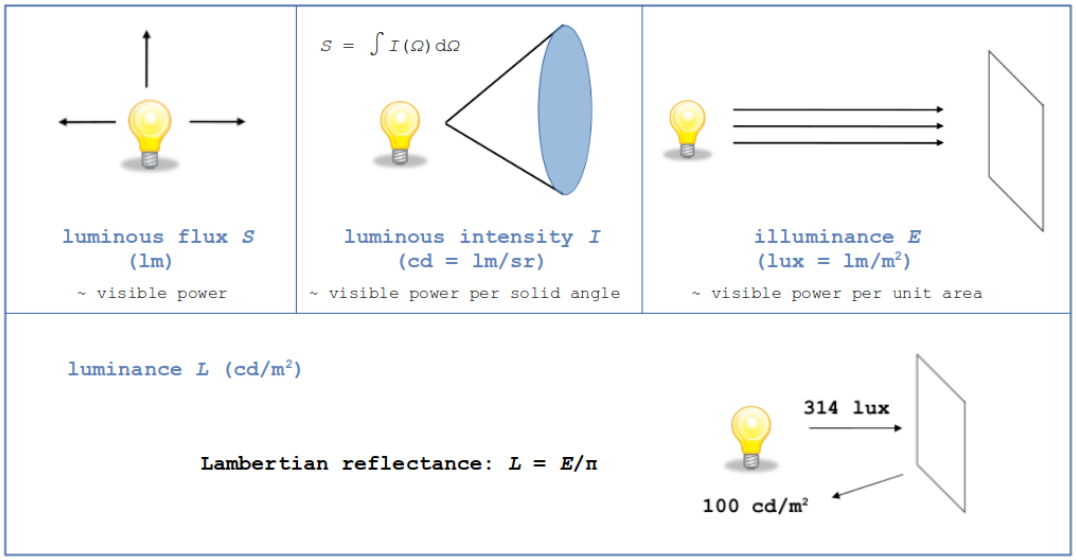

Figure 4.3: Photometric quantities and units.

The corresponding quantities (units) for radiation are radiant flux (W), radiant intensity (W/sr), irradiance (W/m^2), and radiance (W/sr/m^2). The corresponding Dutch names of the photometric quantities are lichtstroom, lichtsterkte, verlichtingssterkte, and luminantie.

4.2 Retinal illuminance

The amount of light that reaches the retina does not only depends on the luminance of the observed object, but also on the pupil diameter. For this reason, visual scientists use a quantity called retinal illuminance with unit troland (Td). Retinal illuminance can be calculated by multiplying the luminance L in cd/m^2 by the pupil area in mm^2 (note: a pupil with a diameter D has an area $\pi D^2/4$, hence, retinal illuminance equals $L\pi D^2/4$). The pupil diameter of the human eye ranges from approximately 8 mm in darkness to 2 mm at high luminances. As such, adjustment of the pupil diameter can only account for a small part of the adaptation of the eye to luminance differences during the day (Table 4.1).

Table 4.1: Some examples of luminances and corresponding pupil diameters [18] and retinal illuminances

	L (cd/m^2)	D (mm)	retinal illuminance (Td)
starry sky	1×10^{-3}	7	0.04
computer screen	100	2.5	5×10^2
clear sky	8×10^3	2	3×10^4
sun at noon	2×10^9	2	6×10^9

Exercises

1. In the past, the Watt was a useful unit for describing the performance of a light bulb. Why has this been changed? Which quantity and unit are currently used?

2. At 555 nm, that is, at the peak of the V_λ curve (Figure 4.1, left panel), a monochromatic light source of 1 W produces a luminous flux of 683 lm. In fact, this is the way the lumen has been (re)defined (in 1979). What is the luminous flux of a 1 W monochromatic source of 510 nm? And of 400, 610, and 700 nm?

3. The old definition of the lumen was based on the amount of light emitted by a candle. A candle can be considered a point source emitting light uniformly in all directions and has a luminous intensity I of 1 cd (that's where the name candela came from...). What is the luminous flux S of this light source?

4. What is the difference between a mirror and a Lambertian surface? A light bulb, which may be considered a point source, with a luminous flux of 220 lm is positioned 2 m from a white-painted wall (in good approximation a Lambertian surface). What luminance would you expect to measure if you direct a luminance meter to the wall? Is the distance between the luminance meter and the wall influencing the observed value?

5. In the previous exercise, the measured luminance value appeared to be clearly higher than the calculated value. What could be the reason(s) for the observed discrepancy?

6. What is the illuminance E at a distance of 4 m from a candle (or tea light)? At 4 m, there is a Lambertian surface. What is the luminance coming from this surface (you may ignore the confounding factors identified in the previous exercise)? What is the retinal illuminance if you would look at the surface with a pupil diameter of 7 mm?

7. Over how many log units of luminance is the human eye able to function? And of retinal illuminance?

8. Why does the spectral sensitivity of the human eye differ from the absorptance spectra of the visual pigments in the photoreceptor cells?

Chapter 5

Color vision

Human color vision starts with the fact that the retina contains three different types of cones, which are named long, middle, and short wavelength cones, or red (R), green (G), and blue (B) cones. Figure 5.1 shows the spectral sensitivity of the three cone types. Note that (1) the human eye is more sensitive to red and green light than to blue light and (2) the spectral sensitivities of the three cone types show considerable overlap.

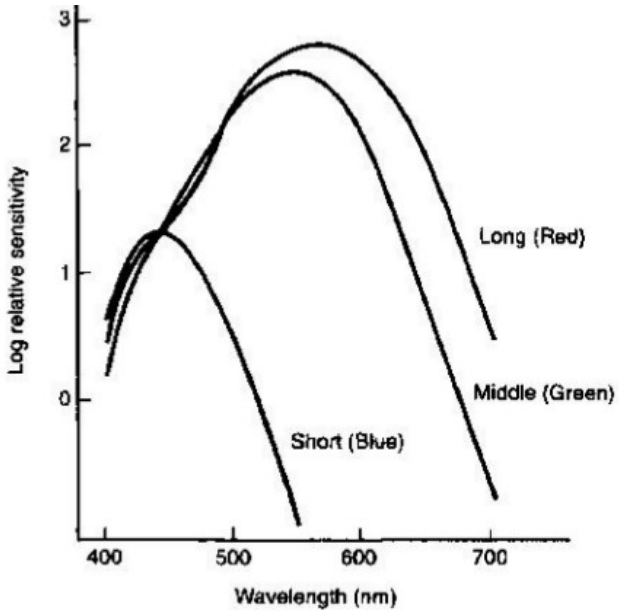

Figure 5.1: Spectral sensitivity of the three cone types.

Any color can be observed when the output of three monochromatic light sources is combined, assuming that the three light sources each stimulate predominantly a different cone type (red, green, and blue). Although some modern lamps produce white light by mixing the light from a red, green, and blue LED, most light sources have a more complex emission spectrum. Figure 5.2 shows the emission spectra of some (formerly) common light sources.

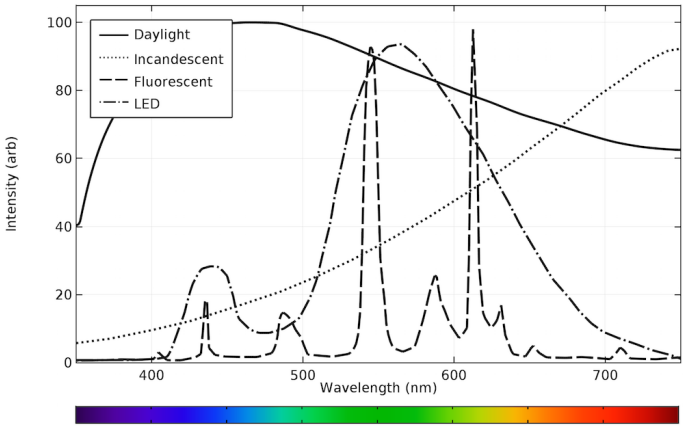

Figure 5.2: Emission spectra of some common light sources.

5.1 From light source to perceived color

In order to be able to determine the color perceived by a human observer for any light source, the CIE (Commission Internationale de l'éclairage or International Commission on Illumination) developed, in 1931, a mathematical framework that links the emission spectrum $I(\lambda)$ of a light source to a unique color. The framework is based on the physiology of color vision. In this framework, the spectral sensitivity of the red, green, and blue cone are standardized and called tuning curves (Figure 5.3).

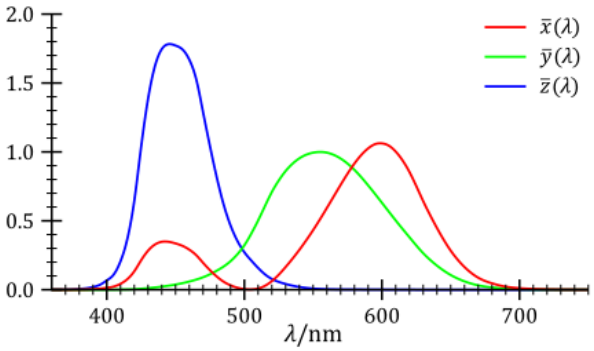

Figure 5.3: CIE 1931 tuning curves.

For a light source with emission spectrum $I(\lambda)$, the CIE primaries X, Y, and Z represent the output of the red, green, and blue cone, respectively, and are given by:

$$X = \int_{400}^{700} I(\lambda)\bar{x}(\lambda)\, d\lambda \tag{5.1}$$

$$Y = \int_{400}^{700} I(\lambda)\bar{y}(\lambda)\, d\lambda \tag{5.2}$$

$$Z = \int_{400}^{700} I(\lambda)\bar{z}(\lambda)\, d\lambda \tag{5.3}$$

where $\bar{x}(\lambda)$, $\bar{y}(\lambda)$, and $\bar{z}(\lambda)$ represent the red, green, and blue tuning curve, respectively (Figure 5.3). Subsequently, the so-called color coordinates (x, y) can be calculated from the three CIE primaries:

$$x = \frac{X}{X + Y + Z} \tag{5.4}$$

$$y = \frac{Y}{X + Y + Z} \tag{5.5}$$

Finally, the perceived color can be found in the chromaticity diagram (CIE 1931 color space; Figure 5.4). For example, for $(x, y) = (0.5, 0.4)$, the perceived color is orange.

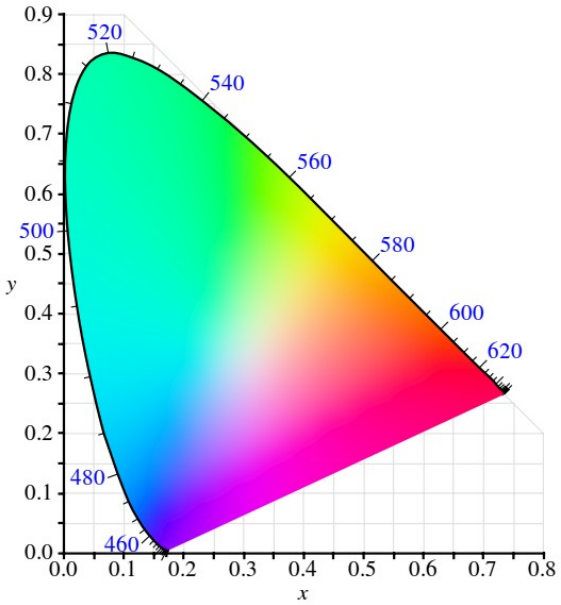

Figure 5.4: Chromaticity diagram.

5.2 Black-body radiation

Any heated object emits EM radiation with a specific emission spectrum that depends only on the temperature of the object: black-body radiation. If the temperature is relatively low (3000 K), red dominates the spectrum ('red hot'; 'roodgloeiend'); if the temperature is relatively high (6000 K), all colors are present similarly ('white hot'; 'witheet'). Figure 5.5 presents black-body radiation spectra for several temperatures. Examples of black-body radiation are a candle (1800 K), a light bulb (incandescent lamp; 2700-3300 K), and daylight (6500 K). In a light bulb,

a filament is heated by an electric current; in the case of daylight, the surface of the sun acts as the heated object.

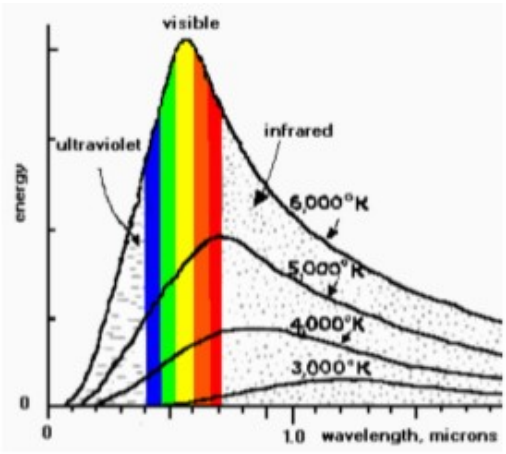

Figure 5.5: Black-body radiation spectra.

For black-body radiation (Figure 5.5), the emission spectrum $I(\lambda)$ is given by:

$$I(\lambda, T) = \frac{2\pi hc^2}{\lambda^5} \frac{1}{e^{hc/\lambda kT} - 1} \tag{5.6}$$

where λ is the wavelength, T the absolute temperature, h Planck's constant, c the speed of light, and k the Boltzmann constant. If we substitute Eq. (5.6) in Eqs. (5.1)-(5.3) and the resulting X, Y, and Z subsequently in Eqs. (5.4) and (5.5), and we finally plot the resulting (x, y) as a function of T in the chromaticity diagram, then it is clear that, for black-body radiation, temperature is one-to-one entangled with color: color temperature (Figure 5.6).

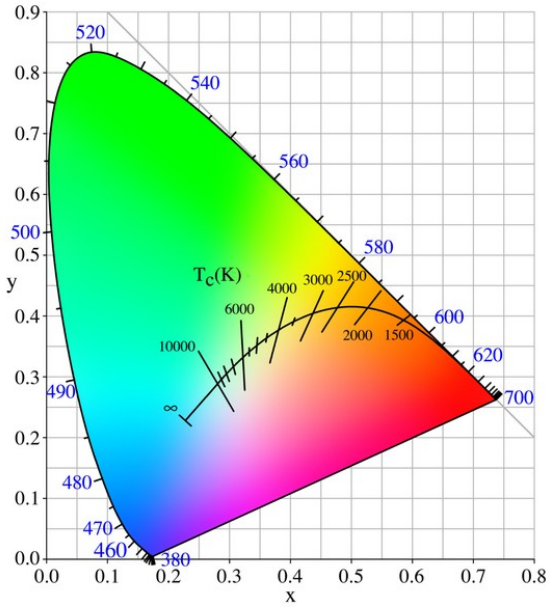

Figure 5.6: Color temperature defined in chromaticity diagram.

5.3 Color blindness and color vision tests

Color blindness in humans is nearly always congenital and is caused by the missing or the malfunction of one (or more) cone types. The inheritance is X-recessive, implying that the majority of color blind people are male. About 8% of the males is affected; the most common defect is a defective or missing green cone ('deutan'), followed by a defective or missing red cone ('protan'). Blue cone related color blindness ('tritan') is rare. Subjects with a deutan, protan, or tritan defect have a normal visual acuity, contrast sensitivity, and visual field, and they can also discriminate most of the colors, but they make certain mistakes. In fact, they have a dichromatic rather than a trichromatic visual system.

If we have two light sources with emission spectra that yield, when using Eqs. (5.1)-(5.3), the same X and Z but different Y, then they can be discriminated by subjects with normal color vision but not by subjects with a deutan defect. Similarly, two different light sources that yield the same Y and Z but different X cannot be discriminated by subjects with a protan defect. This is the basis of color vision tests. Figure 5.7 (left panel) shows one plate of the Ishihara test, by far the most commonly used color vision test. Subjects with normal color vision report 26, with a deutan defect 2, and with a protan defect 6.

Figure 5.7: Left: One plate of the Ishihara test. Right: Farnsworth D15 test.

Another commonly used test is the Farnsworth D15 test (Figure 5.7, right panel). Here, 15 colored caps have to be sorted, starting with a fixed (16th) reference cap. The design of this test is left as an exercise.

Appropriate illumination of color vision tests is important: color vision disappears at low luminances (rods take over the photoreception at scotopic luminances; cones only function at photopic luminances) and the spectral composition of the light reflected from the tests obviously depends on the emission spectrum of the applied light source. Practically, a luminance of 100 cd/m^2 and a color temperature of 6500 K (dedicated light source or daylight at noon with a cloudy sky) are appropriate. A poor light source (from the point of view of luminance or emission spectrum) may result in false-positive test results.

Exercises

1. Calculate the color coordinates (x, y) if all the cone types have the same output ($X = Y = Z$). What is the corresponding color?

2. The emission spectra of three different light sources result in an output of the red, green, and blue cones of:

$$\begin{bmatrix} X \\ Y \\ Z \end{bmatrix} = \begin{bmatrix} 1 \\ 0.5 \\ 1 \end{bmatrix} \text{ (source 1), } \begin{bmatrix} 1 \\ 1.5 \\ 1 \end{bmatrix} \text{ (source 2), and } \begin{bmatrix} 2.5 \\ 1.5 \\ 1 \end{bmatrix} \text{ (source 3).}$$

Which two sources are mixed-up by a subject with a deutan defect? And which two sources by a subject with a protan defect? Calculate the color coordinates (x, y) of these three sources, and plot them in the chromaticity diagram (Figure 5.4).

3. Confusion lines are lines in the chromaticity diagram that connect colors that are mixed-up by color blind subjects. Draw a line for $X = 1$ and $Z = 1$, for Y ranging from 0 to 2. This is confusion line 1. Draw another line (confusion line 2), now for $Y = 1$ and $Z = 1$, and X ranging from 0 to 2. Which confusion line belongs to deutan?

4. Draw a circle with radius 0.1 and center (0.33,0.33) in the chromaticity diagram of the previous exercise. If you divide the circumference of the circle in 16 equal parts, you have - approximately - the colors as used in the D15 test. Which colors are mixed-up by subjects with a deutan defect? And by subjects with a protan defect?

5. If both you and your uncle are color blind, but your parents are not, is the uncle a brother of your mother or of your father? What percentage of women is color blind?

Chapter 6

Tonometry (including pachymetry)

The eye is a hollow structure filled with a fluid. The fluid (aqueous humor) is produced by the ciliary body and leaves the eye through the trabecular meshwork. Inflow and outflow are equal: the volume of the eye is essentially constant over time. The production/inflow of the fluid (approximately 8 ml per 24 hour) is almost independent of the intraocular pressure (IOP); the outflow depends on the pressure gradient (IOP minus the venous pressure outside the eye) and the outflow resistance. As a consequence, an increase in outflow resistance results in an increase in IOP. An elevated IOP threatens the neural tissue in the eye. Especially the axons of the retinal ganglion cells, which constitute the optic nerve, are vulnerable. An IOP related degeneration of the optic nerve is called glaucoma. Glaucoma is an age-related chronic eye disease that may result - if left untreated (lowering of the IOP through medication, laser treatment, or surgery) - in blindness. It affects approximately 2% of the elderly population. An assessment of the IOP - tonometry - is part of a regular eye examination and aims to uncover glaucoma or evaluate its treatment. The mean IOP in healthy eyes is approximately 15 mmHg with a standard deviation of 3 mmHg.

Three commonly used tonometer principles will be discussed here: Goldmann applanation tonometry (GAT), impact-rebound tonometry (ICARE), and non-contact tonometry (NCT).

6.1 Goldmann applanation tonometry (GAT)

GAT is currently the most widely used technique for measuring IOP by ophthalmologists in their consulting room, and is considered to be the gold standard for measuring IOP. After instilling a drop of oxybuprocaine for anesthesia, a probe with a flat front surface (diameter 3.06 mm) is gently pressed against the cornea. Aim is to flatten the cornea over a standardized area; the force needed for the flattening is a measure of the IOP. This is based on the Imbert-Fick law:

$$P = F/A \tag{6.1}$$

where P is the pressure within the sphere and F the external force needed to flatten the sphere over an area A. The Imbert-Fick law assumes that the surface is perfectly spherical, dry, thin, and flexible. This is not the case for the eye: an additional force is needed to deform the cornea and a force has to be subtracted because of the surface tension of the tear film. These two forced are assumed to annihilate each other.

Figure 6.1 shows GAT. During the tuning of the force with the 'adjustment knob', the amount of flattening is observed through a biprism. The visibility is facilitated by coloring the tear film with fluorescein and the use of blue light. In the three examples, the dial reading equals the IOP (left), is higher than the IOP (middle), and is lower than the IOP.

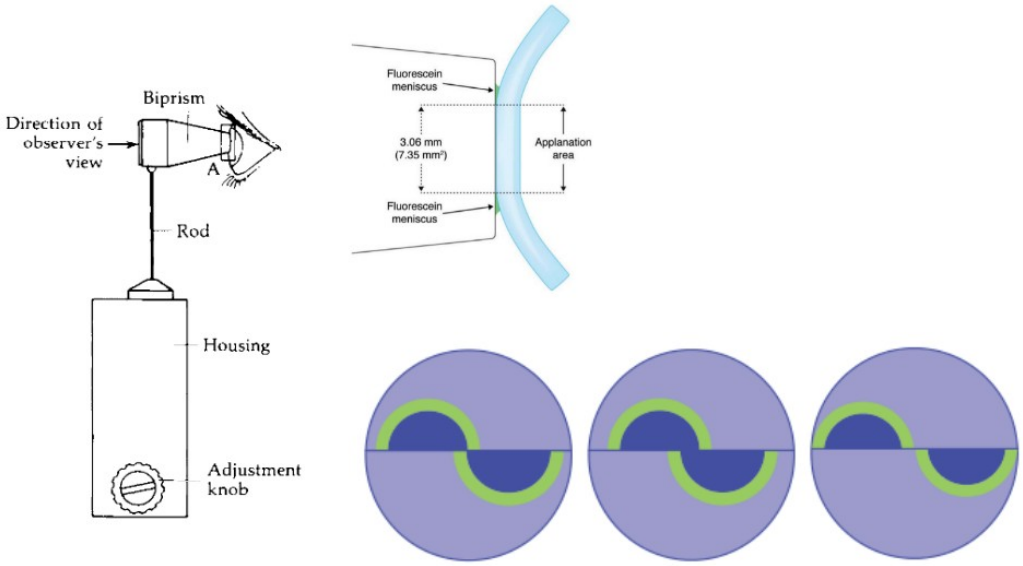

Figure 6.1: Goldmann applanation tonometry: device, principle, and readings.

6.2 Impact-rebound tonometry (ICARE)

The ICARE tonometer (Figure 6.2; left panel) uses the impact-rebound principle as originally developed in Groningen by Dekking and Coster in 1967 (Figure 6.3) [3]. A small probe containing a permanent magnet is launched towards the eye using a solenoid. The probe impacts with the cornea (Figure 6.2; right panel) and rebounds. The same solenoid, inside which the probe moves, is used to measure the movement of the probe, by measuring the induction current produced by the moving magnet. In its current form, produced by a Finnish company, it is a handheld tonometer. As the ICARE tonometer is, unlike GAT and NCT (see next section), a portable device, it is especially useful for bedridden or wheelchair-bound patients, for young children, and in the operating room and other settings outside the consulting room.

Figure 6.2: ICARE tonometer in action (left) and probe impacts the eye (right).

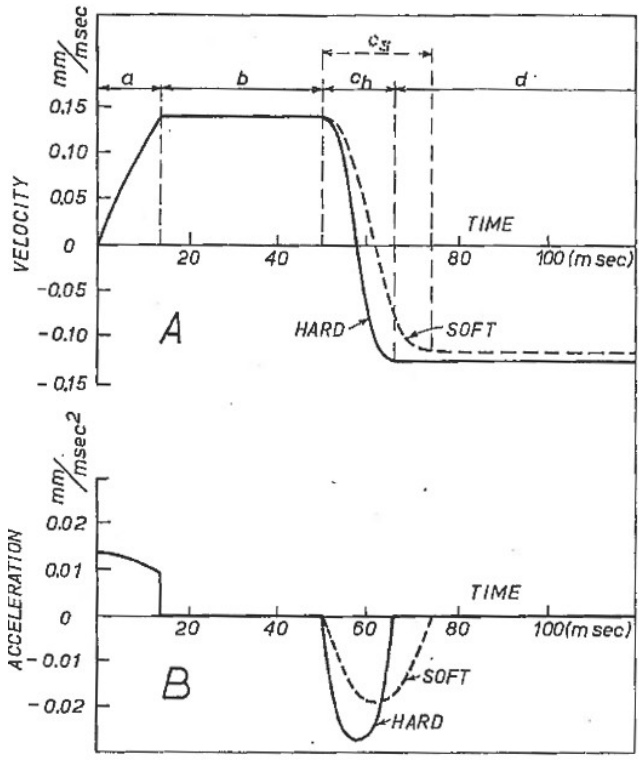

Figure 6.3: Physics underlying impact-rebound tonometry [3].

6.3 Non-contact tonometry (NCT)

NCT ('air-puff tonometry') is the default technique in the optician shop. Figure 6.4 depicts the underlying physics. A stream of air (B) is blown against the cornea and its flow increases until the resulting deformation of the cornea yields a flat mirror. Once flat, the cornea reflects the collimated beam of light (light whose rays are parallel) coming from the transmitter (T) as a collimated beam (as opposed to a diverging or converging beam in case of a convex or concave mirror) that is focused on the detector (D) by a lens in the receiver (R). The pinhole aperture (A) in front of the detector ensures that only in case of a perfectly flat cornea (an thus a perfectly collimated beam in the receiver arm), a significant amount of light enters the detector. When the detector is activated by the reflected light, the air stream is switched off and the corresponding flow is converted into an IOP value. NCT can be used without anesthesia.

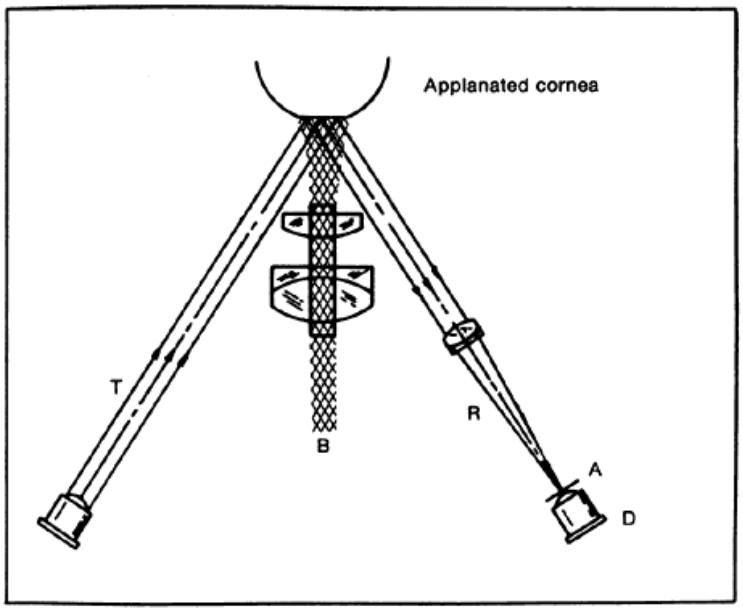

Figure 6.4: Principle of air-puff tonometry (NCT) [6].

6.4 Pachymetry

The thickness of the cornea influences the IOP measurement. In case of a thick cornea, the IOP is overestimated; in case of a thin cornea, it is underestimated. The average central corneal thickness (CCT) is approximately 550 μm; the CCT ranges in the population from approximately 500 to 600 μm. The CCT related IOP measurement error is approximately 5 mmHg per 100 μm. CCT can be measured with either ultrasonography ('ultrasound pachymetry'; Figure 6.5) or with interferometry. Both techniques are described in Chapter 9.

Figure 6.5: Ultrasound pachymetry.

Exercises

1. For GAT, a force corresponding to a mass of 1 g corresponds (on earth) to an IOP of 10 mmHg. What is the area of the surface flattened during applanation tonometry?

2. Describe Figure 6.3. At what time point (1) stops the current that accelerates the probe, (2) does the probe touch the cornea, (3) does the probe reverse, and (4) leaves the probe the cornea?

3. Sketch the output of the detector (D) in Figure 6.4 (y-axis) as a function of the air flow (x-axis). The x-axis should range from 0 to a value amply exceeding the flow that yields a locally flat cornea. What is the focal length of the lens in the receiver?

4. Why is default A-scan ultrasonography as used for axial length assessment (Chapter 9) not suitable for pachymetry? And why is it not possible to use a pachymeter for axial length assessment?

Chapter 7

Fundus photography

The fundus (the inside, back surface of the eye) can be observed and photographed via the pupil. Fundus photography aims to detect and document pathology of the retina. Figure 7.1 shows a normal retina (upper left), a retina with macular degeneration (upper right), diabetic retinopathy (lower right), and a glaucomatous optic nerve head (ONH; lower left).

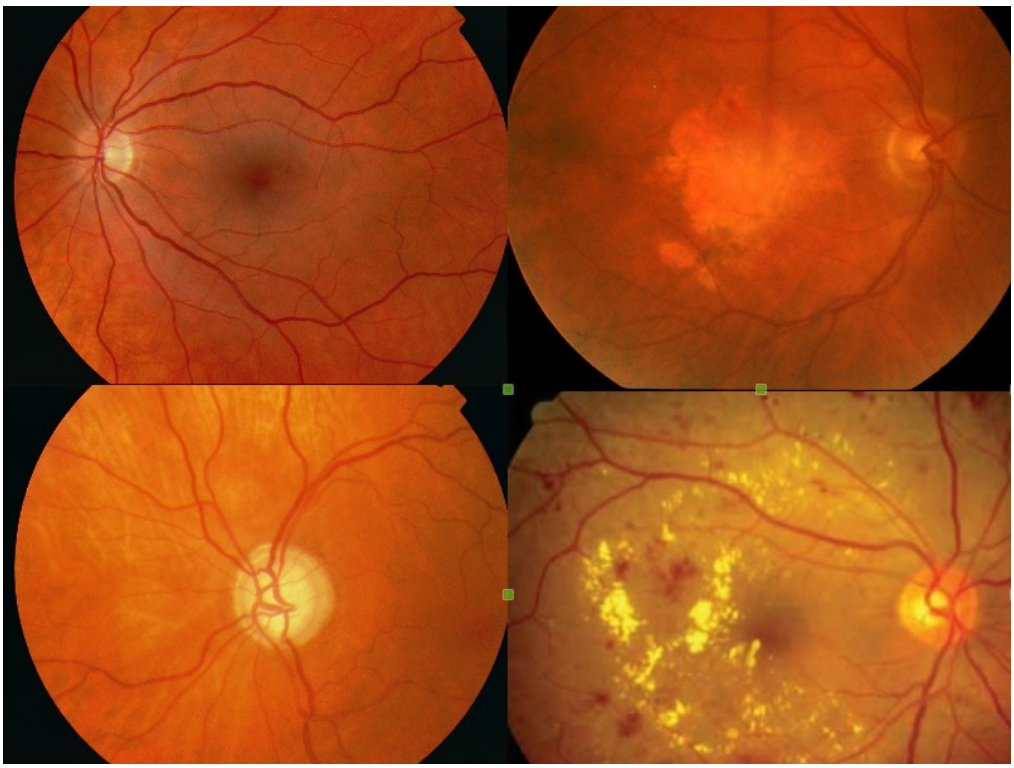

Figure 7.1: Examples of fundus pictures.

7.1 Fundus camera

Basically, a fundus camera is a camera connected to a funduscope (ophthalmoscope). A funduscope is a device used by an ophthalmologist to observe the retina. In its most basic form a funduscope consists of a single positive lens (condensing lens or condensor) and a light source to illuminate the retina. The optics of the eye (cornea and lens) and the condensing lens together form an astronomical telescope (Figure 7.2). An upside down image of the retina is formed in between the condensing lens and the observer (at the 'intermediate image plane'). This image can be observed directly (Figure 7.3, left panel; the hand-held device in the left hand is the light source; the condensing lens is in the right hand) or through a microscope ('biomicroscopy'; Figure 7.3, right panel).

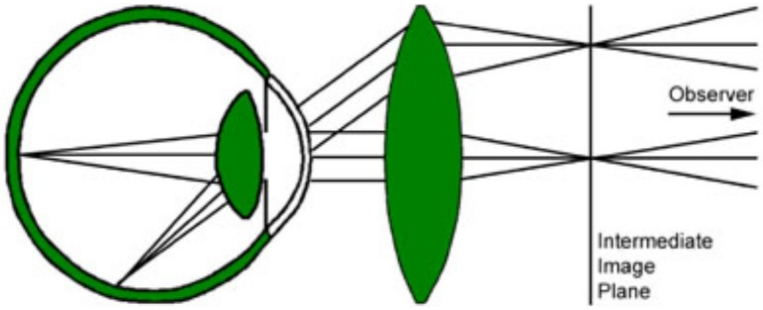

Figure 7.2: Funduscope principle.

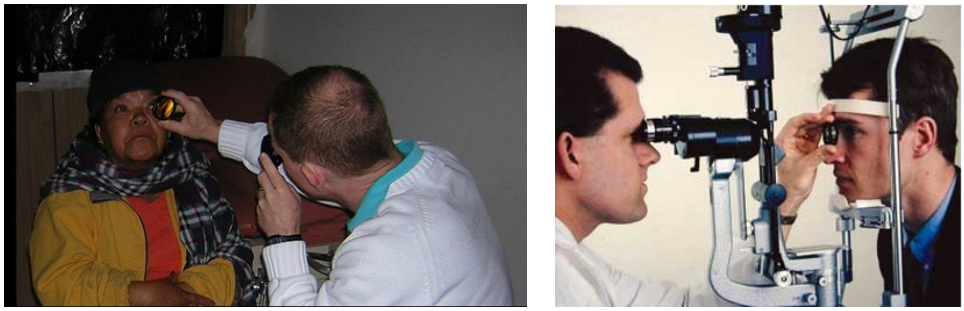

Figure 7.3: Funduscopy (left) and biomicroscopy (right).

Figure 7.4 shows the principle of a fundus camera. It consists of two telescopes, yielding an upright image of the retina at the level of the photographic film (or - nowadays - CCD chip). Halfway the second telescope, the light source comes in.

The spectral distribution of the light source can be controlled with a color filter. This is especially useful in fluorescein angiography (FAG). In this technique, fluorescein sodium is injected in a vein, travels trough the circulation to the eye and, when illuminated with blue light (480 nm), emits green light (525 nm). With a green filter in front of the camera, only the emitted light reaches the camera. Both the (blue) excitation filter and the (green) barrier filter are interference band-pass filters. With FAG, both occluded and leaking retinal vessels can be diagnosed. Figure 7.5 shows a FAG of a normal eye (left panel: the arteries are already filled with fluorescein but the veins not yet; right panel: both the arteries and the veins are filled with fluorescein).

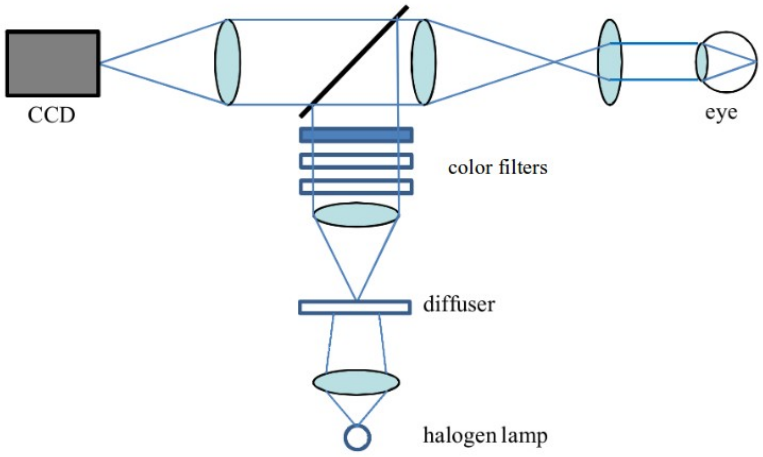

Figure 7.4: Principle of fundus camera.

Some pathological retinal structures show fluorescence without the need of injecting fluorescein sodium: autofluorescence.

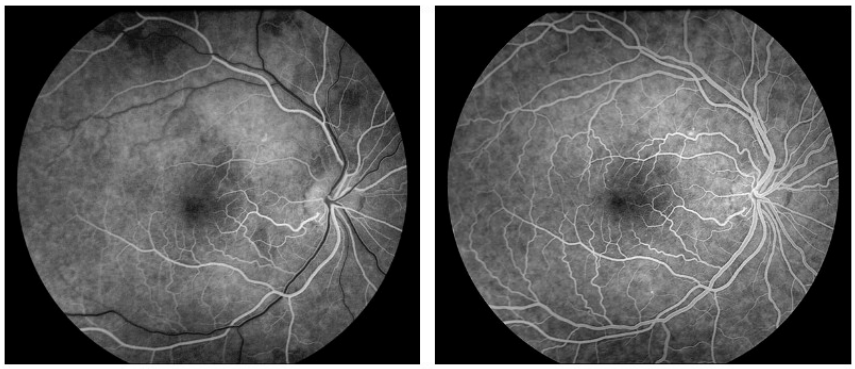

Figure 7.5: Fluorescein angiography (arterial and venous phase).

7.2 Confocal scanning laser ophthalmoscope (CSLO)

Figure 7.6 shows the principle of CSLO. The retina is scanned with one or more laser beams. Only the rays that are reflected from the aimed location at the focal plane (continuous lines in Figure 7.6) are able to pass the confocal aperture and reach the detector. This results in an image that is not cluttered by light reflected before or after the focal plane (dashed lines).

Commercially available as OPTOS wide-field camera, CSLO uses two laser wavelengths, green (532 nm) and red (635 nm), to produce color images. By a special scanning system, wide-field images of approximately 180-200° are possible (Figure 7.7; cf. 45° with conventional fundus photography). A third, blue laser (488 nm) is available for fluorescein angiography (see above); a fourth, infrared laser (802 nm) for indocyanine green angiography.

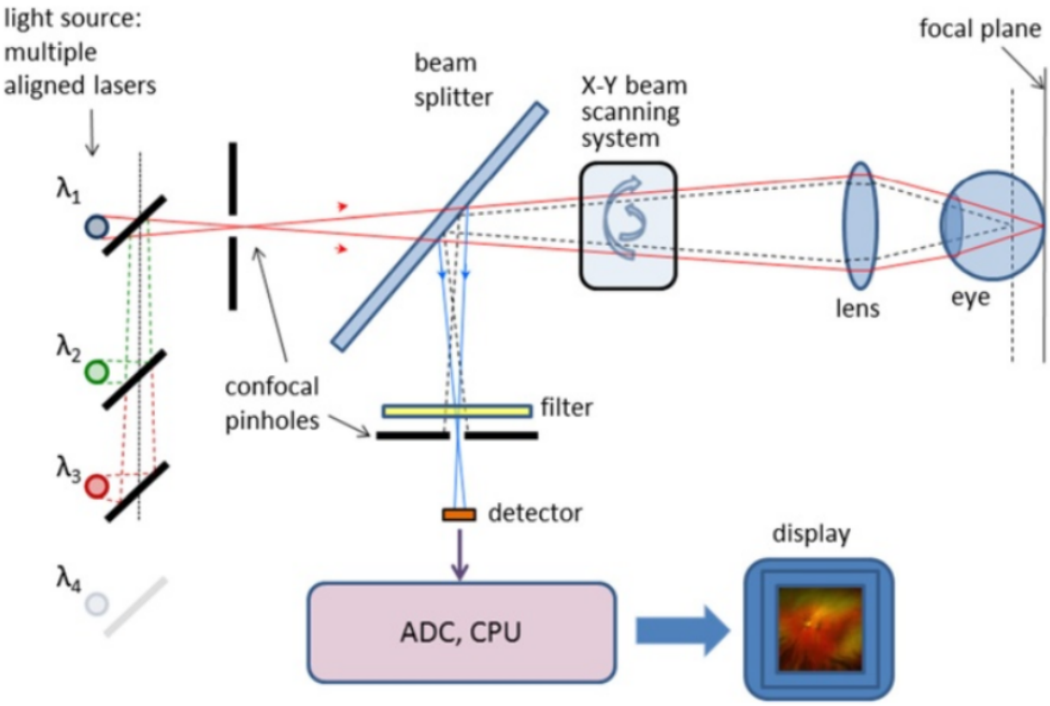

Figure 7.6: Principle of confocal scanning laser ophthalmoscopy (modified from [8]).

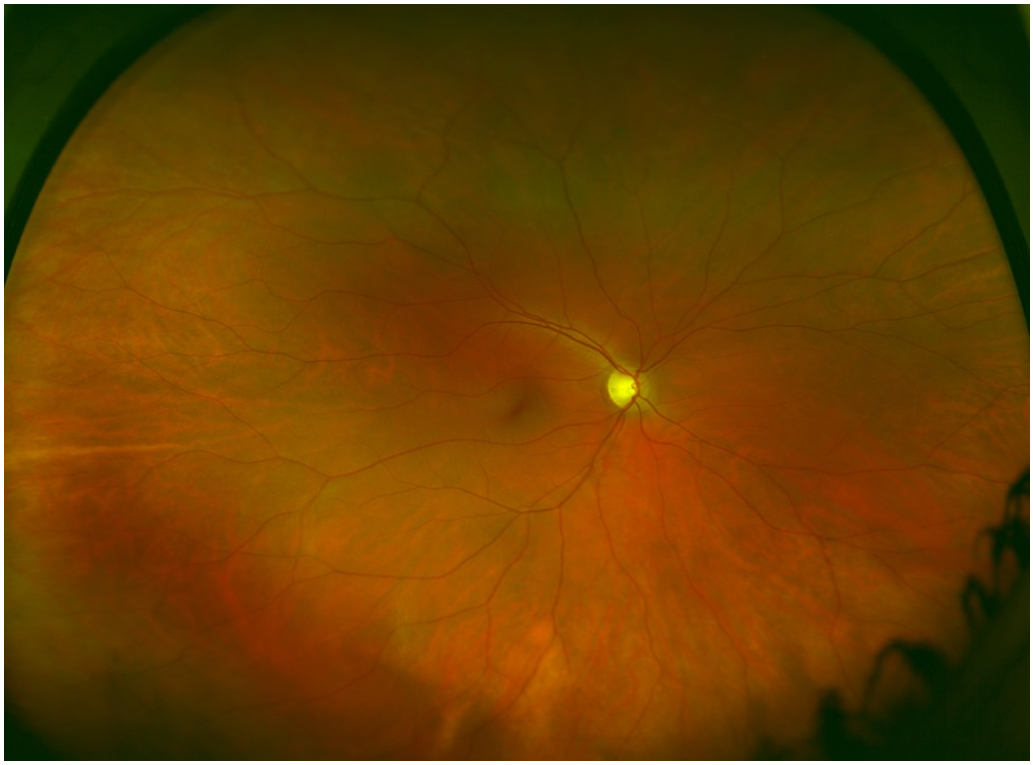

Figure 7.7: CSLO image from OPTOS wide-field camera.

Exercises

1. Why is an astronomical telescope considered an afocal optical system?

2. A simple funduscope (Figure 7.2) consists of a condensing lens that forms - together with the optics of the eye - an astronomical telescope. The power of the optics of the eye is 60 D; the condensing lens is 20 D. The diameter of the optic nerve head (ONH) is 1.5 mm. What is the size of the image of the ONH that is formed in between the condensing lens and the observer? What is the distance between the condensing lens and the image? Is the image upright or upside down?

3. With biomicroscopy, a condensing lens of 90 D is used together with a 10× magnifying microscope. What is the overall magnification?

4. Fluorescence/luminescence is the emission of light by a substance that has absorbed light or other electromagnetic radiation. Luminescence of indocyanine green can be induced by infrared radiation of typically 800 nm. The emitted radiation will have a wavelength of:

A. 525 nm
B. 800 nm
C. 830 nm

5. What does angiography with indocyanine green add to angiography with fluorescein sodium?

Chapter 8

Optical coherence tomography

Optical coherence tomography (OCT) is an imaging technique introduced in ophthalmology in 1991 [10]. It enables the visualization of the deeper layers of the retina, which cannot be imaged with fundus photography. Figure 8.1 shows a fundus image (left panel) and an OCT scan (right panel). This particular scan comprises a slice perpendicular to the retinal surface, located at the blue line in the left panel.

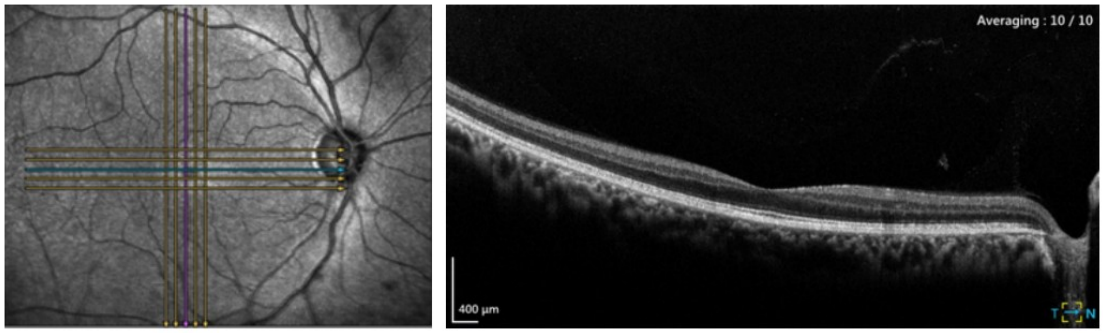

Figure 8.1: Example of OCT scan (right) and corresponding fundus image (left).

OCT is often considered as 'ultrasonography with light'. However, there is a fundamental difference. In ultrasonography, structures are localized on the basis of time differences between emitted and received ultrasound. Light (or better: IR radiation) goes a way too fast to measure time differences on a μm to cm scale. For that reason, the localization of structures with light needs a different physical principle (see below). Another difference between ultrasonography and OCT is spatial resolution. Figure 8.2 shows an ultrasound image of the eye; the retina can be seen clearly because it is detached (a pathological condition). Clearly, the spatial resolution of ultrasonography is much lower than that of OCT (right panel of Figure 8.1).

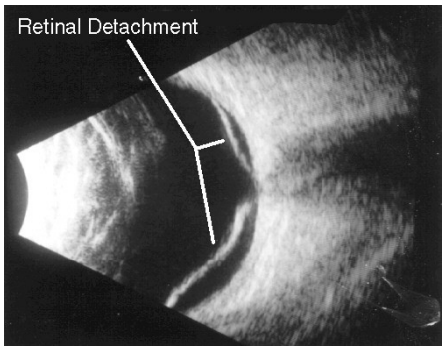

Figure 8.2: USG B-scan of the human eye with retinal detachment.

8.1 General principles of OCT

The physics underlying OCT is interferometry, and as such OCT dates back to 1887, to the famous experiment of Michelson and Morley [12]. Figure 8.3 shows the basic principle of interferometry. Light from a single source is divided in two beams that interfere with each other after being reunited. The interference pattern, and - relevant to OCT - especially the central intensity of this pattern, depends on the difference in path length traveled by the two beams.

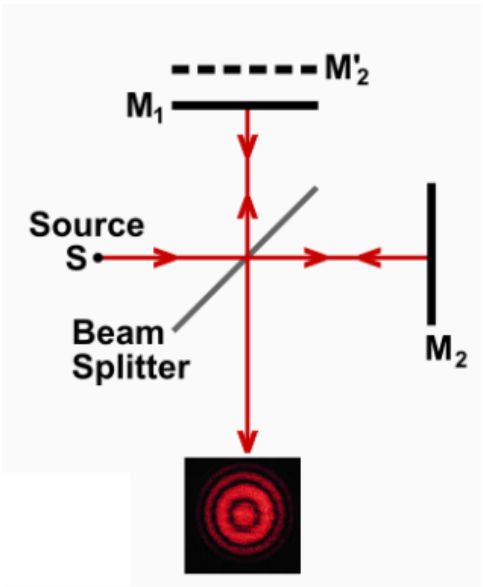

Figure 8.3: Principle of interferometry (modified from https://en.wikipedia.org/wiki/Interferometry). Note: the circular interference fringes only occur with monochromatic light and path length difference $\neq 0$.

Figure 8.4 presents the two-slit experiment of Thomas Young, for monochromatic and white light. The crucial difference is that monochromatic light yields a repetitive interference pattern whereas white (broadband) light yields only interference if the path length difference between the two pathways is close to zero. Hence, if you want to measure absolute distances with interferometry, you need a broadband light source: low-coherence interferometry.

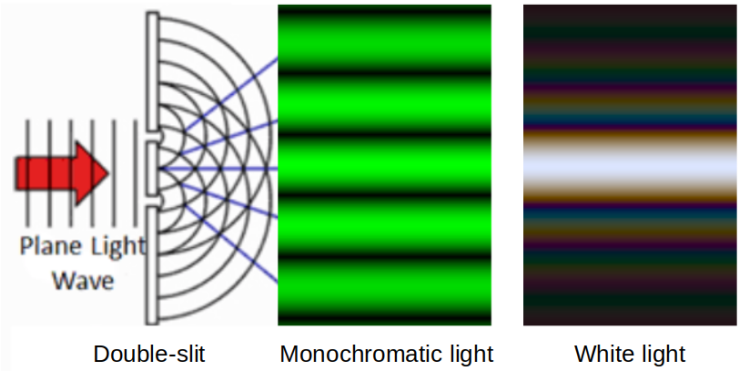

Figure 8.4: Two-slit experiment with monochromatic and white light.

The path length difference over which interference occurs in the case of a broadband light source is called the coherence length l_c. The broader the bandwidth $\Delta\lambda$ of the source, the smaller l_c:

$$l_c = 0.88\frac{\lambda_0^2}{\Delta\lambda} \tag{8.1}$$

where λ_0 is the wavelength corresponding to the peak of the spectral distribution of the source. This is illustrated in Figure 8.5. The axial resolution of interferometry (the accuracy with which you can determine the mirror position) is determined by the coherence length, and - following the Rayleigh criterion - equals $l_c/2$. The factor 2 originates from the fact that if you change the position of a mirror, the optical path length changes twice that distance.

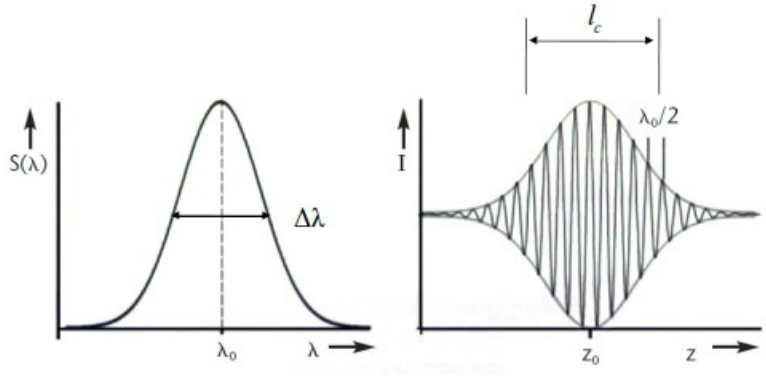

Figure 8.5: Low-coherence interferometry. Coherence length l_c equals the FWHM of the envelope; $\Delta\lambda$ equals the FWHM of the power spectrum of the light source $S(\lambda)$.

An interferometer contains two mirrors (M1 and M2 in Figure 8.3); in OCT, one mirror is called the reference mirror, the other mirror is formed by backscatter (reflectance) due to inhomogeneities in refractive index in the retina (left panel of Figure 8.6).

By measuring the signal strength at the detector while moving the reference mirror, the tissue reflectance can be measured along a line perpendicular to the retinal surface: A-scan (right panel of Figure 8.6). By introducing a rotating mirror (Figure 8.7; 'lateral scan'), an array of adjacent A-scans can be assessed, yielding a cross-sectional image: B-scan (right panel of Figure 8.1).

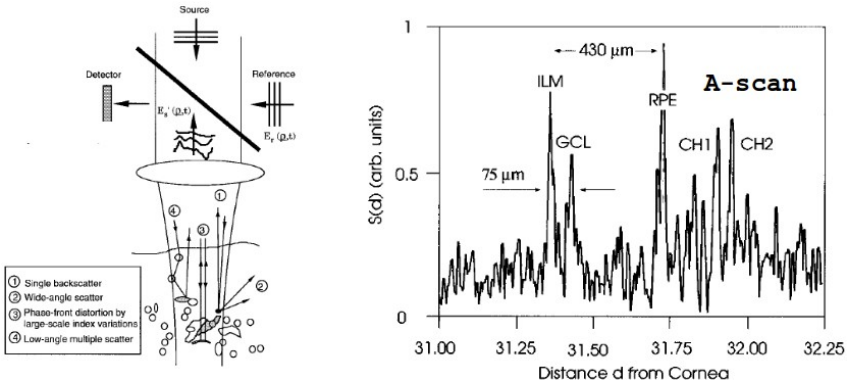

Figure 8.6: OCT: backscatter (left [16]) and A-scan (right [4]).

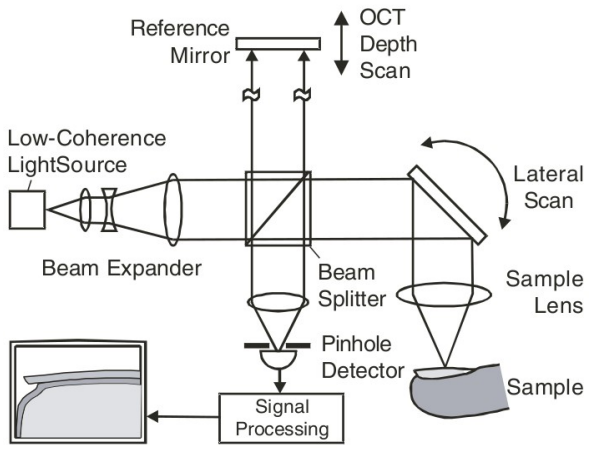

Figure 8.7: OCT: B-scan [5].

8.2 Time-domain versus spectral-domain OCT

Instead of using a moving reference mirror (time-domain (TD) OCT; Figure 8.7 and left panel of Figure 8.8), an A-scan can also be produced by using a fixed reference mirror together with a spectrometer (spectral-domain (SD) OCT; right panel of Figure 8.8). The spectrometer consists of a reflection grating, a positive lens, and a line scan camera (single CCD array).

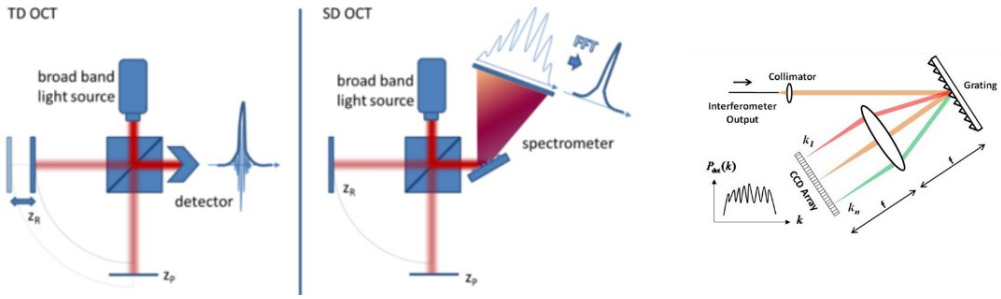

Figure 8.8: Time-domain (left) and spectral-domain (right) OCT.

Figure 8.9 shows how depth information can be retrieved from white light interference together with a spectrometer. The first column shows the original interference pattern; the remaining

four columns are examples of interference patterns of monochromatic colors that together form the broadband light source. With zero path length difference between reference mirror and object ($z = 0$), all colors are in phase and this yields white light. For any non-zero path length difference ($z \neq 0$), some colors are in phase and others are not. As a consequence, each $|z|$ has a unique color coding. Note that, for each value of z, z and -z have the same color coding. Hence, the total output consists of an image and a corresponding mirror image (left panel of Figure 8.10). Clinical devices present only half of this image ($z > 0$ or $z < 0$). However, if the sample crosses $z = 0$, the mirror image pops up as an artifact (right panel of Figure 8.10).

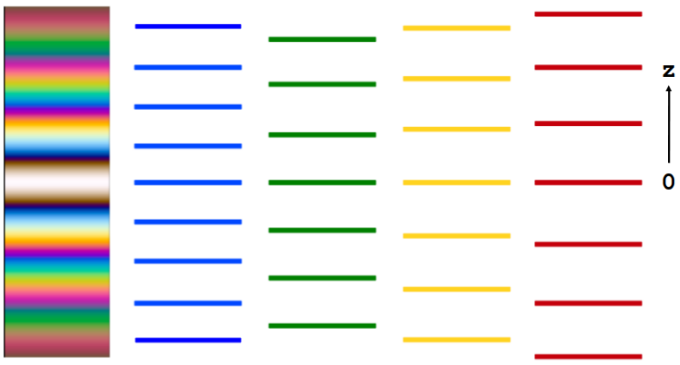

Figure 8.9: Depth information from color.

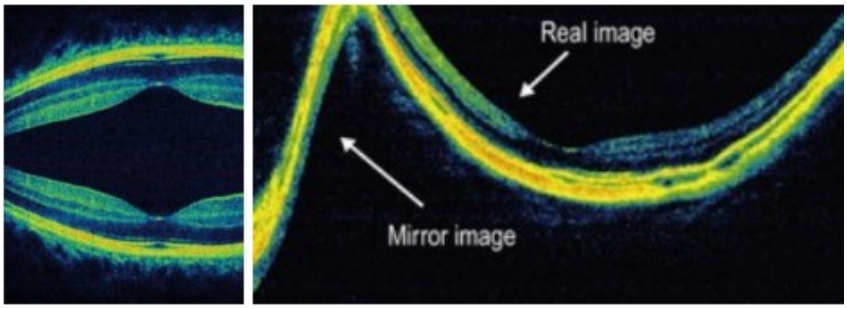

Figure 8.10: Mirror image: as a logical result of the underlying physics (left) and as seen by the clinician as an artifact (right).

Mathematically, the depth information is retrieved from the spectrometer output by using a (inverse) Fourier transform (that's why SD OCT is also called Fourier domain (FD) OCT).

Signal-to-noise ratio

Figure 8.11 shows an SD and a TD OCT B-scan of the same part of the retina (foveal area). As can be seen in this figure, the signal-to-noise ratio (SNR) of SD OCT is greater than that of TD OCT. One reason for this difference in SNR is that in SD OCT the entire axial range (A-scan) is sampled in a single measurement, which implies a better SNR for a given acquisition time (in TD OCT, an A-scan consists of a series of measurements interrupted by a change of the position of the reference mirror). Another reason is that noise in OCT is mainly white noise, which - in SD OCT - distributes itself over the various spectrometer channels in an uncorrelated way.

In contrast to this, the signal pieces that are distributed over the channels may be considered correlated. Hence, in the SNR calculation, the pieces in the numerator are added before squared and in the denominator squared before added. Finally, the theoretical axial resolution equals $l_c/2$ in TD OCT (see above) and $l_c/4$ in SD OCT (see below, 'Advanced OCT physics').

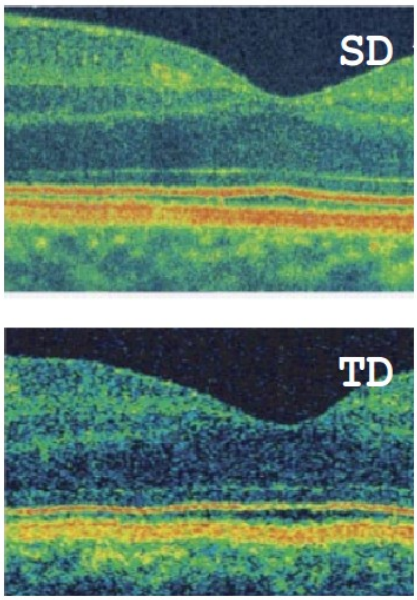

Figure 8.11: Noise in SD (top) and TD (bottom) OCT (modified from [21]).

8.3 Clinical applications

Current clinical use of the OCT is twofold. Either B-scans can be assessed by the clinician directly in a qualitative way (by looking at the images) or sophisticated quantitative analysis is performed before the data are presented to the clinician. A qualitative assessment is common in diseases of the macula. Figure 8.12, for example, shows a healthy foveal area (left) and a foveal area with cystoid macular edema (CME; right).

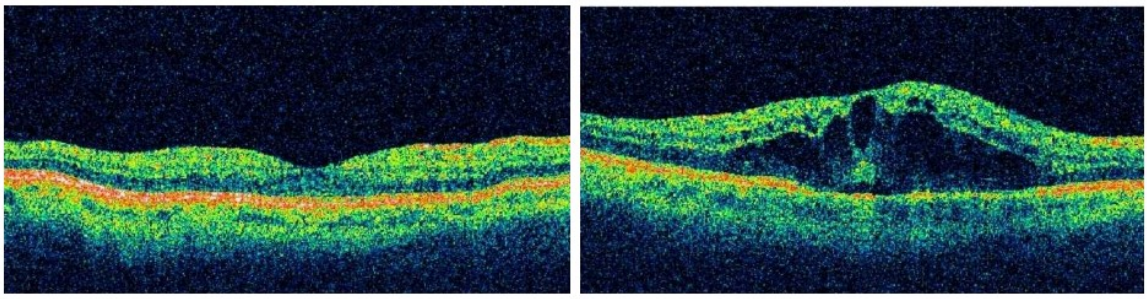

Figure 8.12: Retina with cystoid macular edema (right) and normal retina (left).

For glaucoma, a disease characterized by a thinning of the retinal nerve fiber layer (RNFL) and retinal ganglion cell layer (RGCL), a cube scan (a series of B-scans) is performed around the optic nerve head and in the macular area (Figure 8.13).

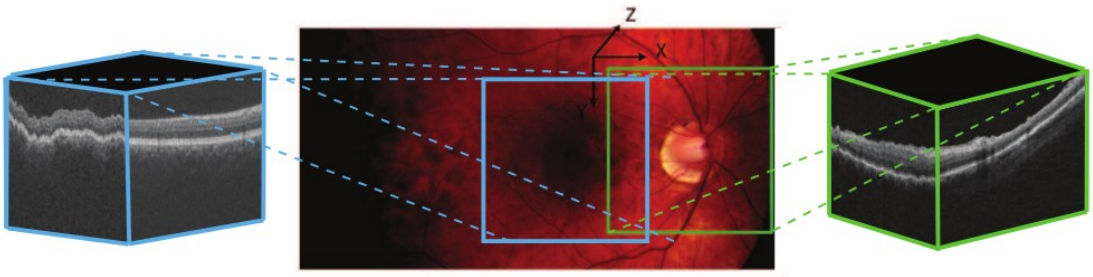

Figure 8.13: OCT cube scans of macular (left) and optic nerve head (right) area.

Different cell types reflect (backscatter) light differently. Dedicated software ('segmentation software') is able to detect these differences and to delineate the borders between the different cell layers, thus enabling the calculation of cell layer thicknesses. The thicknesses are presented to the clinician in a convenient way (Figures 8.14 and 8.15). This example shows a patient with a glaucomatous right eye and a normal left eye. Figure 8.14 shows, among others, the thickness of the RNFL analyzed in a circle around the optic nerve head. Figure 8.15 presents an analysis of the thickness of the RNFL, RGCL, and inner plexiform layer together, in the macular area. In both figures, a color coding is used to depict a comparison of the patient to a built-in normative database (white: thicker than expected; green: within normal limits; yellow or red: outside normal limits).

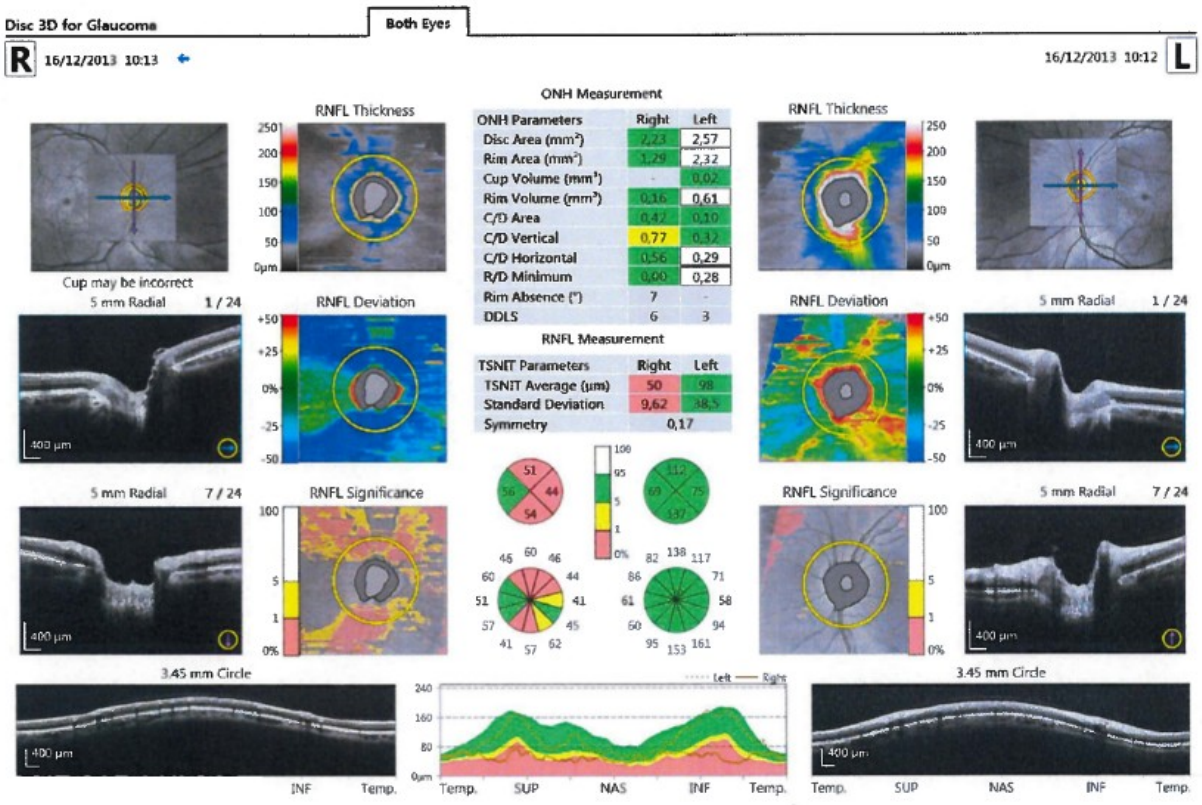

Figure 8.14: Analysis of OCT cube scan of the optic nerve head region. Right eye abnormal (color-coded yellow/red); left eye normal (color-coded white/green).

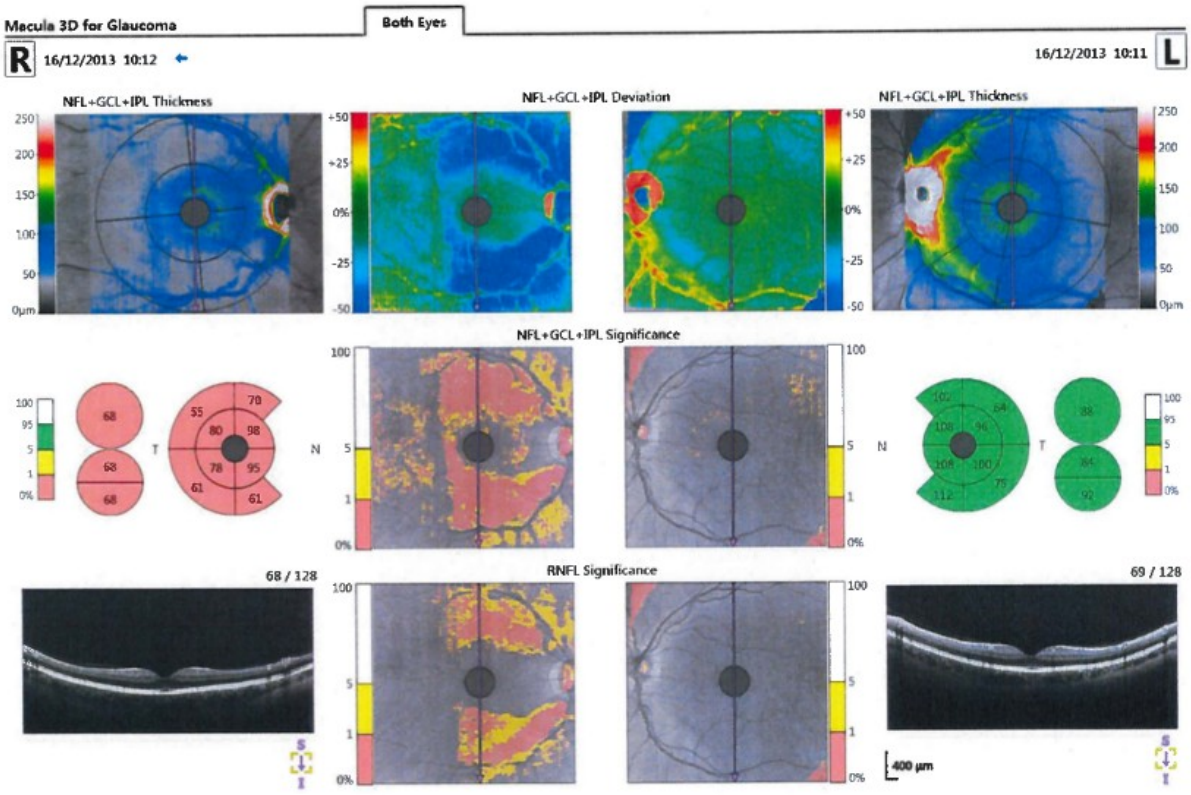

Figure 8.15: Analysis of OCT cube scan of the macular area. Focus is on retinal layers relevant to glaucoma: retinal nerve fiber layer (RNFL), ganglion cell layer (RGCL), and inner plexiform layer (IPL). Right eye abnormal (color-coded red); left eye normal (color-coded green). Thicknesses are presented in μm.

Exercises

1. Calculate the spatial resolution of ultrasonography (Figure 8.2). Assume a frequency of 10 MHz and assume that the spatial resolution equals the wavelength. Be aware that the speed of sound in the eye (1555 m/s) is substantially different from the speed in air.

2. Calculate the coherence length l_c of an OCT light source with a peak wavelength λ_0 of 800 nm and a bandwidth $\Delta\lambda$ of 30 nm. Subsequently, calculate the axial resolution of TD OCT. By what factor differ the axial resolution of OCT and the spatial resolution of ultrasonography (Exercise 1)? What is the thickness of the human retina? Conclusion?

3. What is the range of suitable wavelengths for OCT, if applied to image the human retina in an intact eye? Hint: see Figure 4.2, left panel (Chapter 4). What are - within this range - advantages of short wavelengths and of long wavelengths?

4. See Figure 8.12, left panel. In which direction are the A-scans performed? What is the 'dip' in the middle of the B-scan? Which side is pointing towards the lens and cornea? What do the colors mean?

5. What is the essential difference between TD and SD OCT?
   A. the way the A-scan is acquired
   B. the way the B-scan is acquired
   C. the light source

6. Give two reasons why the SNR of SD OCT exceeds that of TD OCT. What is the impact of this difference in terms of resolution and acquisition time?

7. Where is the 'equal-path length line' in the left and right panel of Figure 8.10?

8.4 Advanced OCT physics

TD OCT

The light intensity as a function of wavenumber entering the detector in the left panel of Figure 8.6, $I(k)$, is given by (at $t = 0$ s, that is, ignoring the temporal component, which is reasonable because light oscillates much faster than any detector can handle):

$$I(k) \sim |E_r + E_s|^2 + |E_r|^2 + |E_s|^2 + 2|E_r \cdot E_s| = |E_r|^2 + |E_s|^2 + 2|E_r||E_s| \cos(k(z_r - z_s)) \quad (8.2)$$

where $E_r(k)$ and $E_s(k)$ (abbreviated as E_r and E_s) are the electric field strength related to the beams with wavenumber k entering the detector from the reference mirror and tissue sample, respectively, and $z_r - z_s$ the optical path length difference. Integration over k yields:

$$I \sim I_r + I_s + 2\sqrt{I_r I_s} g(z_r - z_s) \quad (8.3)$$

where I_r and I_s are the intensities related to the beams entering the detector from the reference mirror and tissue sample, respectively, and $g(z_r - z_s)$ the interference pattern as displayed in the right panel of Figure 8.5. The peak of the envelope of $g(z_r - z_s)$ coincides with zero optical path length difference ($z_r - z_s = 0$).

The intensity I at the detector consists of a 'DC' component, $I_r + I_s$, and an 'AC' component, $2\sqrt{I_r I_s} g(z_r - z_s)$. The reflectance of the human eye is very small: most of the light is absorbed in the retina (that's why our pupils look black). Hence, $I_r \gg I_s$ and thus the photons from the reference beam form the major component of the detector input. The reflectance of the eye can be studied by removing the DC component by high-pass filtering the detector output while moving the reference mirror. As I_r is constant and I_s proportional to the reflectance of the eye,

the AC component is proportional to the square root of the reflectance. Given that the output of a photodiode or CCD cell is proportional to its input I, the output has to be squared to get a signal that properly represents reflectance.

With I_r being the major component of the detector input, the major source of noise in OCT is shot noise (Poisson photon noise) from the reference beam. As shot noise is essentially white noise, it survives the DC removal. Shot noise can be reduced by increasing the detector integration time. Obviously, this compromises the overall scan time.

With $F(k)$ being the spectral distribution of the low-coherence light source as displayed in the left panel of Figure 8.5, but now described in k-space instead of λ-space, we get for the interference pattern $g(z_r - z_s)$:

$$g(z_r - z_s) \sim \int_{-\infty}^{\infty} F(K) e^{ik(z_r - z_s)}\, dk \tag{8.4}$$

Hence, $g(z_r - z_s)$ is the Fourier transform of $F(k)$. If we approximate $F(k)$ by a Gaussian function with standard deviation σ_k centered around k_0 we get:

$$g(z_r - z_s) \sim e^{ik_0(z_r - z_s)} e^{-(z_r - z_s)^2 \sigma_k^2/2} \tag{8.5}$$

for which we used the property that the Fourier transform of a Gaussian function is also a Gaussian function, with $\sigma = 1/\sigma_k$, and a shift over k_0 in k-space yields $e^{ik_0(z_r - z_s)}$ in the transform. The first part of Eq. (8.5), $e^{ik_0(z_r - z_s)}$, depicts the interference; the second part, $e^{-(z_r - z_s)^2 \sigma_k^2/2}$, the low-coherence envelope - together they form a 'wave packet'. With coherence length l_c being the FWHM of the wave packet (Figure 8.5), we get:

$$l_c = \frac{2\sqrt{2 \ln 2}}{\sigma_k} \tag{8.6}$$

It is left as an exercise to show that this is equivalent to Eq. (8.1).

The most likely position of the wave packet (that is, the location of the maximum of its probability distribution $|g(z)|^2$) is given by:

$$\langle z \rangle = \int_{-\infty}^{\infty} z |g(z)|^2\, dz \tag{8.7}$$

where $z = z_r - z_s$ is the optical path length difference. Eq. (8.7) yields $\langle z \rangle = 0$ (z is an uneven and $|g(z)|^2$ an even function), that is, the probability distribution has its maximum at $z_r = z_s$.

SD OCT

First, the spectrometer output, which is equally spaced in λ, has to be rescaled to be equally spaced in wavenumber k, with $k = 2\pi/\lambda$. The reflectance of the sample R_s as a function of z can subsequently be found by taking the inverse Fourier transform of $I(k)$ as given in Eq. (8.2), which results in the desired A-scan and serveral other terms:

$$|FT^{-1}[I(k)]|^2 \sim \Gamma^2(z) * \{I_r^2\delta(0) + I_s^2 O(z) + I_r I_s A + I_r I_s A_m\} \tag{8.8}$$

where Γ is the envelope of the coherence function (see Figure 8.5), $I_r^2\delta(0)$ the DC component resulting from the beam entering the detector from the reference mirror (with δ the Dirac delta function), $I_s^2 O(z)$ coherence noise, and $I_r I_s A$ and $I_r I_s A_m$ terms proportional to the desired and the mirrored A-scan (see Figure 8.10), respectively. Using the square of the modulus of $FT^{-1}[I(k)]$ ensures an A-scan proportional to the sample reflectance (as I_s is proportional to the reflectance). Figure 8.16 shows the result of the inverse Fourier transform.

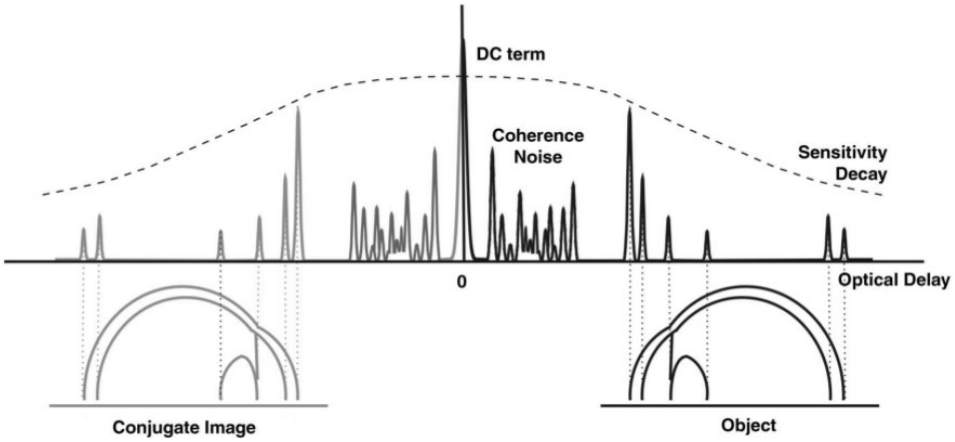

Figure 8.16: Inverse Fourier transform of $I(k)$. The transform contains an A-scan, a mirrored A-scan, a DC component, and coherence noise [20].

The convolution with the coherence function depicts that the axial resolution is limited by the coherence length, as is the case in TD OCT, and also explains why the DC component $I_r^2\delta(0)$ appears wider than a Dirac delta function. Coherence noise results from interference between photons reflected by different layers of the sample; if the sample would consist of only one layer, as in the original interferometer, this term would be a DC component, $I_s^2\delta(0)$, similar to the DC component from the reference beam. The easiest way to get rid of coherence noise is to ensure that $I_r \gg I_s$. This is the case in ophthalmology, as even the highly-reflective retinal layers reflect only a minority of the photons. $I(k)$ is a real function. The (inverse) Fourier transform of a real function is an even function. This is another way to understand Figure 8.10. The desired A-scan and the mirrored A-scan are the two halves of a single, even function. The 'mirror' is located at the equal-path length line ($z = 0$) and either $z > 0$ or $z < 0$ is presented. As the DC

component appears as a large peak at $z = 0$, $z = 0$ itself should not be part of the displayed image.

Figure 8.17 illustrates the Fourier transform. Upper half: a mirror, or any single object causing backscatter, can be considered a delta function in z-space, which corresponds to a periodic function in k-space (connected by the Fourier transform). The peaks of the periodic function represent colors for which the beams reach the spectrometer in phase, that is, the optical path length difference is $n\lambda$, with n an integer. Similarly, the valleys represent the colors for which the path length difference is $(n + \frac{1}{2})\lambda$. Lower half: objects at different positions in z-space yield periodic functions in k-space with different frequencies. A higher frequency in k-space implies a greater path length difference (larger n).

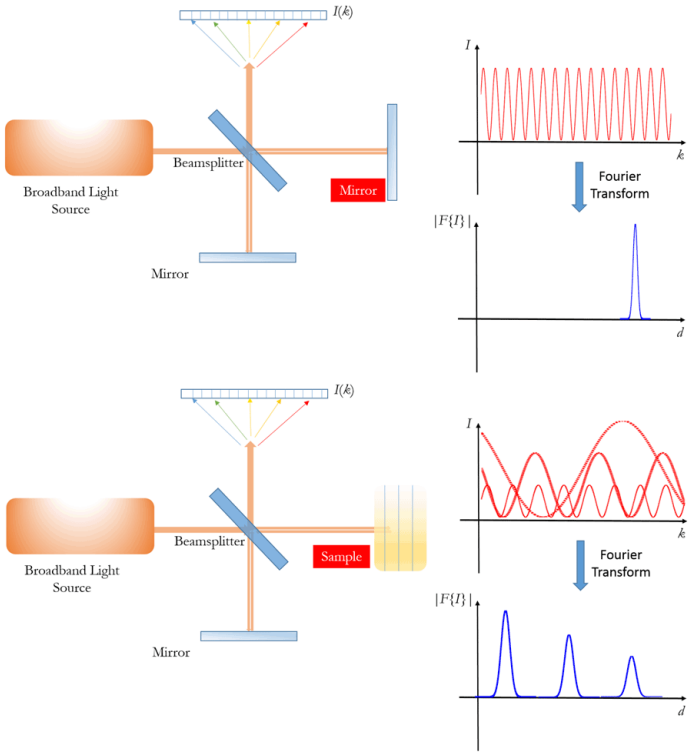

Figure 8.17: From spectrum in k-space to A-scan.

Axial resolution and range

The smaller the distance between the colors dk in the spectrometer, the larger the axial range Δz. This follows directly from the Fourier transform property:

$$\Delta z = 2\pi/dk \tag{8.9}$$

Note that this range includes the image and the mirror image, and the beam goes twice trough the eye. Hence, the effective range is four times smaller: $\pi/(2\,dk)$.

The range in k-space $N\,dk$, with N being the number of pixels of the CCD array in the spectrometer, determines the resolution in z-space dz:

$$dz = \frac{2\pi}{N\,dk} \tag{8.10}$$

Obviously, the spectrometer should be able to capture all the colors that are emitted by the light source. Hence, it should be able to handle at least $2\Delta\lambda$, with $\Delta\lambda$ the bandwidth (FWHM) of the light source (Figure 8.5). Combining Eqs. (8.1) and (8.10) gives:

$$dz = \frac{\lambda^2}{2\Delta\lambda} \approx \frac{l_c}{2} \tag{8.11}$$

Hence, as is the case in TD OCT, also in SD OCT the axial resolution is determined by the coherence length of the light source, and now equals $l_c/4$. The additional factor 2 added to Eq. (8.11) originates - again - from the fact that the beam makes a round trip through the eye.

How many pixels are needed for the CCD array in the spectrometer? The higher the better seems logic but this is not the case, because the computer has to calculate 10,000-100,000 A-scans per second, that is, has to perform 10,000-100,000 Fourier transforms per second. The computational effort of a single fast Fourier transform (FFT), depicted by the number of multiplications, equals $\frac{N}{2}\log_2 N$. Hence, the number of multiplications equals 2304, 5120, and 11264 for N is 512, 1024, and 2048, respectively. For a given light source that spans $\Delta k = N\,dk$, a larger N implies a smaller dk and thus, according to Eqs. (8.10) and (8.9), an unchanged dz together with a larger Δz. The human retina has a thickness of approximately 300 μm. However, the retina is curved and sometimes the image is somewhat tilted. For that reason, the effective range should be at least 1-2 mm to get an OCT device that is useful in ophthalmology. The effective range is covered by half of the pixels, that is, $N/2$. Hence:

$$\frac{N}{2} \cdot \frac{l_c}{4n} \approx 1 - 2 \text{ mm} \tag{8.12}$$

where n is the refractive index in the eye (see next subsection). In modern OCT devices, a typical value of N is 1024. So, if you want to improve the axial resolution of your OCT device, the first step is to select a light source with a larger $\Delta\lambda$ to get a smaller l_c (Eq. (8.1)). The second step is to buy a faster computer and increase N in order to keep the effective range unchanged (Eq. (8.12)).

Refractive index and dispersion

Thus far, the equations (except for Eq. (8.12)) addressed interferometry in air. However, the eye is filled with a substance resembling water, and thus the optical path length is not identical to the physical path length. Hence, to get the effective thicknesses, range, and axial resolution in tissue, the obtained values have to be divided by the refractive index n. For SD OCT this results in $\pi/(2n\,dk)$ for the effective range and $l_c/(4n)$ for the axial resolution. For the eye, $n \approx 1.38$.

The refractive index depends on wavelength. This phenomenon is called dispersion. As a result, the optical path length is different for different colors and this degrades the image quality. In TD OCT, dispersion artifacts can be compensated by putting glass or water in the reference beam. In SD OCT dispersion compensation can also be done numerically.

Lateral resolution

The lateral resolution of both TD and SD OCT is limited by the eye optics. The spatial resolution of the human eye is typically 1 arcmin (Chapter 1), which corresponds to 5 μm on the retina.

Dynamic range

The reflectivity range of the retina is huge. There are two highly-reflective layers: one being the retinal nerve fiber layer (RNFL) and the other consisting of three adjacent highly-reflective layers close to the retinal pigment epithelium (RPE). If we would scale the signal (squared detector output) linearly over the gray scales of a computer display (for an 8-bit display ranging from 0 to 255), then one would see only the highly-reflective layers (left panel of Figure 8.18). Hence, some transform is needed. One option is to take the logarithm of the signal (right panel of Figure 8.18), and express the result in dB after multiplying by 10. Subsequently, the dB values are distributed linearly over the 0-255 display range in such a way that the noise level corresponds to black and the highest possible reflectance (from the RPE) to light gray, close to white but avoiding saturation. For a typical OCT device, the 0-255 range spans about 50 dB.

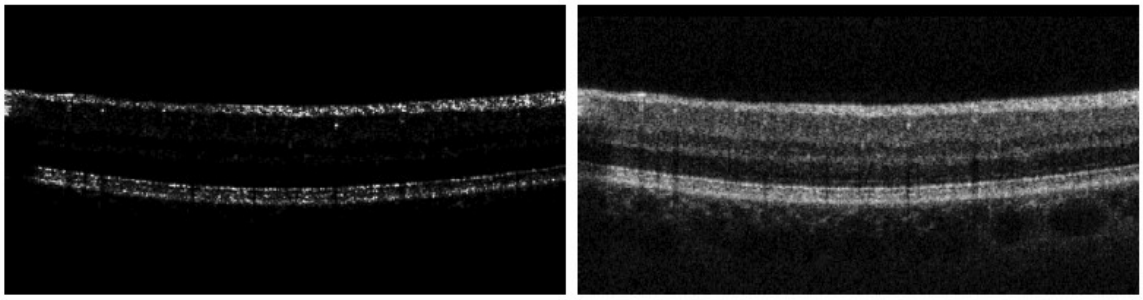

Figure 8.18: Raw squared detector output I^2 (left) and log-transformed image as provided by the device (right; modified from [11]). In the raw image only one high-reflective layer at the top (RNFL) and three adjacent high-reflective layers at the bottom are visible. The log-transformed image uncovers underneath the RNFL: RGCL (gray; retinal ganglion cells), IPL (light gray; amacrine cells), INL (dark gray; bipolar cells), OPL (light gray; horizontal cells), ONL (dark gray; photoreceptor nuclei), external limiting membrane (light gray, very thin), photoreceptor inner segments (dark gray; area with mitochondria), and the three adjacent high-reflective layers: *i.* ellipsoid zone (inner segment to outer segment [area with visual pigment] junction), *ii.* photoreceptor to RPE junction, and *iii.* RPE.

Additional exercises

8. Show that $l_c = 0.88\frac{\lambda_0^2}{\Delta\lambda}$.

9. Show that Eq. (8.1) and Eq. (8.6) are equivalent.

10. What is the Nyquist theorem? What is - in OCT - the low-pass filter that must precede the sampling (a) in axial direction and (b) in lateral direction?

11. Why do the circular interference fringes in Figure 8.3 only occur if the path length difference differs from 0?

Chapter 9

Biometry (axial length assessment and keratometry) and autorefraction

Cataract extraction is the most frequently performed surgical procedure worldwide (in the Netherlands alone more than 100,000 times per year). Cataract is a clouding of the lens of the eye - in most cases it is an age-related disease (Figure 9.1, left upper panel; white pupil). During the cataract extraction, the lens is emulsificated using ultrasound and subsequently removed (right upper panel).

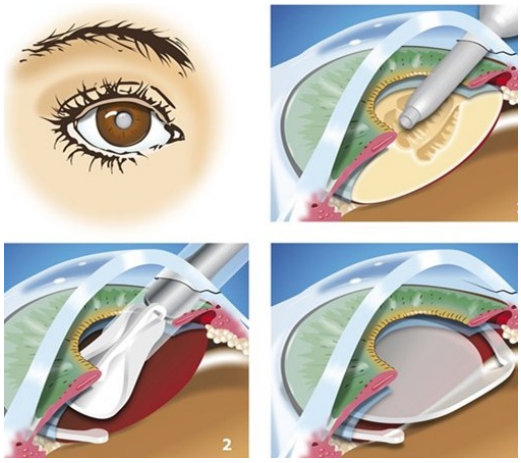

Figure 9.1: Cataract extraction and IOL implantation.

In the early days of the cataract extraction, the cloudy lens was simply removed and the eye was left 'aphakic' (literally: without lens); for clear vision, strong glasses (typically +12 D) or contact lenses (typically +15 D) had to be used. Nowadays, an intraocular lens (IOL) is implanted, yielding a 'pseudophakic' eye (Figure 9.1, lower two panels). An IOL with a power of approximately 22 D implanted in the capsular bag restores the original situation, that is, a preoperatively emmetropic eye (emmetropia: no glasses needed for clear distance vision) remains emmetropic. However, some eyes (with myopia [short-sightedness] or hyperopia [far-

sightedness]) used to need glasses (minus for myopia, plus for hyperopia) for clear distance vision. By measuring some properties of the eye before the operation ('biometry'), the IOL power needed for postoperative emmetropia can be calculated. As a consequence, most pseudophakic patients have clear vision at distance without glasses - they only need reading glasses (an accommodating IOL still has to be invented).

Properties of the eye that influence the IOL power for emmetropia are primarily the corneal curvature K and the axial length L. The corneal curvature K is expressed as a power in D (diopter). A typical value for K is 43 D. A typical value for axial length L is 23 mm.

The oldest formula for IOL power calculations was based on linear regression applied to clinical data and is called the SRK formula. For K in D and L in mm:

$$P = A - 0.9K - 2.5L \tag{9.1}$$

where P is the IOL power in D needed for emmetropia and A a constant. Its value is approximately 118. The SRK formula is now considered outdated, but it is still useful for understanding the effects of K and L.

9.1 Keratometry

The corneal curvature K can be measured with a corneal topograph or with a corneal tomograph. In corneal topography, a set of perfect rings ('Placido's disc') is projected on the cornea; the reflection is analyzed to determine the anterior corneal shape. Figure 9.2 shows a Placido's disc topograph (right), reflection pattern of a healthy cornea (top left), and reflection pattern in a (pathological) condition called keratoconus (bottom left).

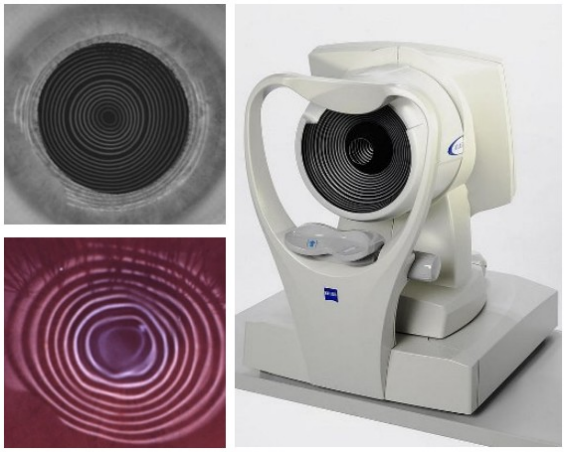

Figure 9.2: Corneal topograph based on Placido's disc.

With the corneal surface acting as a convex mirror, it reflects an object, and a reduced, virtual

upright image is produced. This is illustrated in Figure 9.3. The ratio of the image size and object size is used to estimate the radius R along a particular meridian (assuming $d \gg R$):

$$R = 2dh'/h \tag{9.2}$$

where d is the distance between object and eye, h the object size, and h' the image size. From R, K can be calculated via $K = (n' - 1)/R$, with n' the refractive index inside the eye.

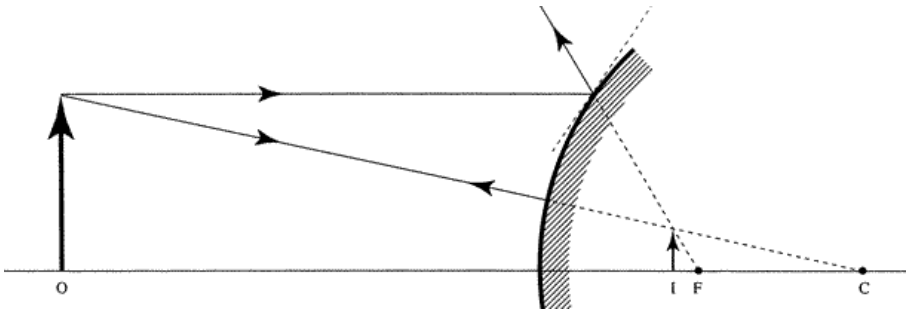

Figure 9.3: A convex mirror produces a reduced, upright image.

In corneal tomography, the Scheimpflug principle is used to make cross-sectional pictures of the cornea without distortion (Figure 9.4). From a series of images made in different meridians, the corneal shape can be determined and subsequently K calculated.

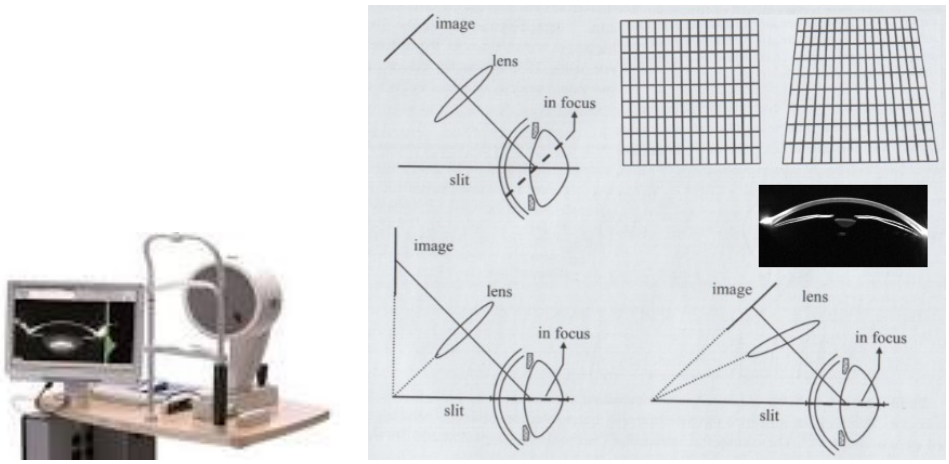

Figure 9.4: Corneal tomography based on Scheimpflug photography. Clinical device (left) and principle (right). In a regular camera, film (CCD chip), lens, and the plane of focus are parallel to each other (right panel, top left). If the lens is tilted with respect to the film, the plane of focus is tilted as well, in such a way that lines through film, lens, and plane of focus intersect in a single point (right panel, bottom left and bottom right). With this configuration, it is possible to take a picture of the cornea with the plane of focus coinciding with the optical axis of the eye (right panel, middle right). In architecture, Scheimpflug photography is used for correcting perspective distortion (right panel, top right).

Ideally, K is the same in all meridians. If not, there is corneal astigmatism, which can be corrected with cylinder glasses. For IOL power calculations in case of astigmatism, the K

value of the steepest and flattest axis (normally these axes are 90° away from each other) are averaged. Toric IOLs are IOLs with different power in orthogonal meridians; they may be used to annihilate corneal astigmatism.

9.2 Axial length assessment

The axial length used to be measured with ultrasonography (Figure 9.5) but is nowadays measured with interferometry (Figure 9.6). The latter technique has a much higher accuracy: the axial resolution of ultrasonography is approximately 0.2 mm at a commonly used frequency of 10 MHz whereas that of interferometry is typically 20 µm. Ultrasonography, however, can - unlike interferometry - be used in the operation room (small children, mentally retarded patients) and in case of dense cataracts. A small systematic error between both techniques exists because ultrasonography measures axial length from the anterior corneal surface to the anterior retinal surface whereas interferometry measures axial length from the anterior corneal surface to the retinal pigment epithelium. A further underestimation of the axial length in ultrasonography may occur if the probe is pressed strongly (as opposed to gently) onto the eye.

Figure 9.5: Axial length measurement through ultrasonography: correct probe placement (left), typical device (middle), and output (right; A-scan: echo signal strength as a function of depth).

The essential difference between optical coherence tomography (Chapter 8) and axial length measurement through interferometry is the presence of a Fabry-Perot interferometer (Figure 9.6). A patient puts his head on the chin rest and looks into the device. The patient has to fixate on the just visible (780 nm) laser beam to assure an accurate, aligned measurement. Distance d in the Fabry-Perot interferometer is adjusted with a stepper motor until an interference pattern (concentric fringes; see Figure 8.3) is observed in the scope or the interference signal strength as measured with the photodetector has reached a maximum. Interference occurs when (twice) the distance d in the Fabry-Perot interferometer and (twice) the optical path length in the eye (axial length L multiplied by the refractive index n' within the eye) are equal, or more exactly, differ by less than the coherence length l_c of the applied laser:

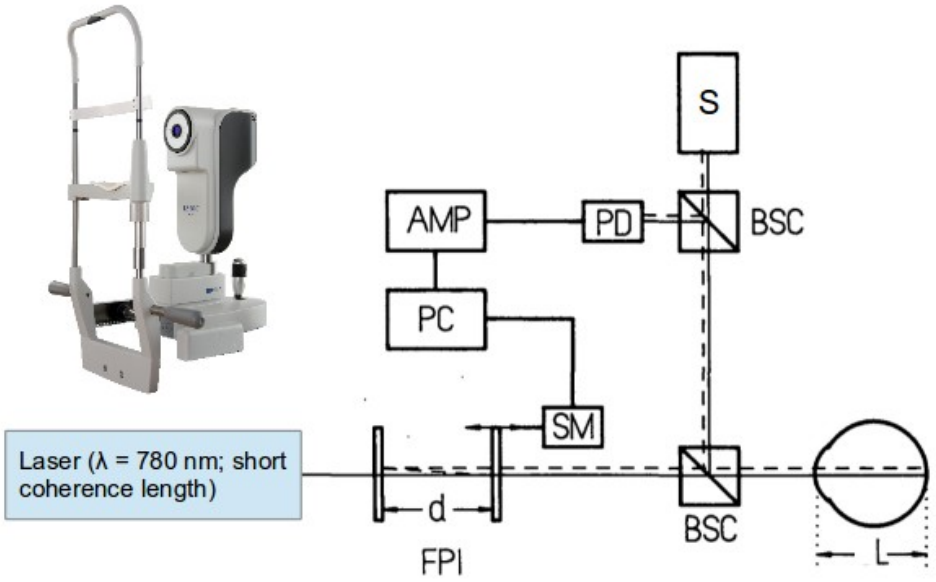

Figure 9.6: Axial length measurement through interferometry. FPI = Fabry-Perot interferometer; BSC = beam splitter cube; S = scope for observer; PD = photodetector; AMP = amplifier; PC = computer; SM = stepper motor (modified from [9]).

$$2|d - n'L| < l_c \tag{9.3}$$

Modern devices have a built-in keratometer and are also able to measure other ocular distances like corneal thickness ('pachymetry'), the distance between the cornea and the lens (anterior chamber depth), and lens thickness. By incorporating these distances, the accuracy of the IOL power calculation may be improved.

9.3 Autorefraction

The refractive state (glasses needed for clear vision at distance) of the eye can be measured with trial lenses by an experienced person, or assessed with an autorefractometer (optometer) device. Figure 9.7 (left panel) shows the principle of such a device: a target is moved in front of a positive lens until a sharp image of the target is projected on the retina. In case of emmetropia (a), the image is sharp if the target is in the front focal plane of the lens. In case of hyperopia (b), the target has to be moved away from the eye in order to get a sharp image, and in case of myopia (c) the target has to be moved towards the eye.

Sharpness of the image can be determined subjectively (in the past) or by an automated optimization of the contrast of the image reflected from the retina (current devices). Another option to determine sharpness is the use of a Scheiner's disc. Scheiner's disc (Figure 9.7, right panel) is

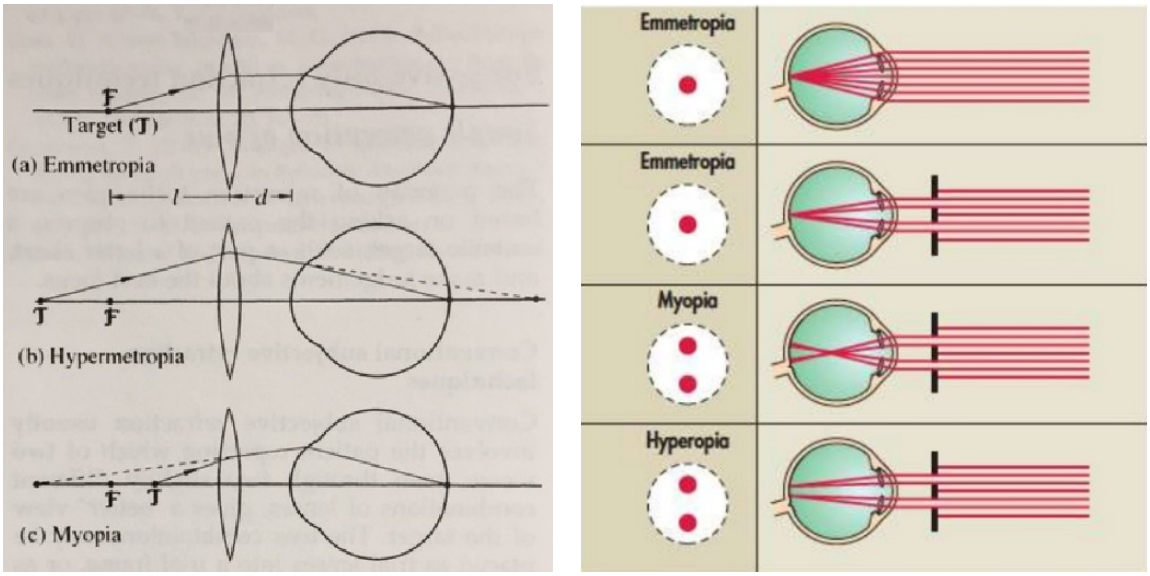

Figure 9.7: Optometer principle (left) and principle of Scheiner's disc (right).

a disc with two small apertures. If placed in front of the eye, a collimated beam will be observed as a single point in case of emmetropia whereas two points are observed in case of either myopia or hyperopia. Now, the vergence of the beam is changed (by moving the target in front of the positive lens) until a single point is observed.

Exercises

1. A myopic patient prefers emmetropia (no glasses for vision at distance) after his cataract extraction. Keratometry shows $K = 43$ D; the axial length measurement yields 27.0 mm. What is the preferred power of the IOL?

2. Keratometry data are presented as a K value in D; however, a corneal topograph or tomograph actually assesses the shape of the anterior corneal surface, and this shape is depicted by the radius R of a sphere fitted to the surface. Calculate R for a corneal surface with $K = 43$ D. You may assume that the refractive index inside the eye, n', equals the refractive index of water.

3. Aphakia can also be corrected with a contact lens. Assume an axial length of 23 mm and a corneal curvature of 43 D. What is the power of the contact lens if the lens is intended for clear vision at distance?

4. Make a ray tracing sketch of a convex mirror with radius R with the object at infinity. Where is the focal point? Where is the image in case of a nearer object? Is it magnified or reduced? Upright or upside down? Show that $R = 2dh'/h$ where d is the distance between object and mirror, h the object height and h' the image height. You may assume $d \gg R$.

5. In Scheimpflug photography, three lines intersect in a single point. Not intersecting in this point is a line running through the:

A. film (CCD chip)

B. lens

C. optical axis

D. plane of focus

6. Potentially, four laser beams may reach the scope in the device of Figure 9.6. Describe these four beams. Two of these beams are supposed to produce together an interference pattern. Which two?

7. Axial length measurement with ultrasonography has a resolution of 0.2 mm, to be compared to 20 μm for interferometry. Is this difference clinically relevant? Hint: what error in IOL power calculation corresponds to an error of 0.2 mm in axial length assessment and what is the resulting refractive error (difference between aimed and needed glasses)?

8. Axial lengths as measured by ultrasound and interferometry differ not only in accuracy but also systematically. How and why?

Chapter 10

Electrophysiology

Vision essentially consists of imaging objects on the retina by the eye optics, capturing the photons by photoreceptor cells (rods and cones), and processing the captured image by retinal neurons and the brain. The photons elicit an electrical signal in the photoreceptor cells, and all subsequent neurons involved in processing and transportation of visual information code this information as electrical signals as well. In animals, these signals can be recorded by inserting micro-electrodes in individual neurons (intracellular recording). In humans, ethics and clinical pragmatism limits recording of visual signals to picking-up mass potentials (that is, the net response originating from an ensemble of photoreceptor cells or neurons that are stimulated simultaneously). Electrodes placed nearby the eye record signals from the retina: electroretinography (ERG); electrodes placed at the backside of the head record signals from the primary visual cortex (striate cortex): visual evoked potentials (VEP; essentially a special case of electroencephalography [EEG]).

10.1 Electrodes and their placement

Figure 10.1 shows the various electrode types and placement. For recording an ERG signal, two electrodes per eye are needed: an active electrode at the front of the eye (practically: a contact lens with integrated electrode, a thin wire [DTL electrode] placed in the lower fornix, or a skin electrode placed directly beneath the eye) and a reference electrode at the rear of the eye (practically: a skin electrode placed at the temporal bone). For recording a VEP signal, at least one active electrode is used. The electrode is placed at the skin of the skull near the visual cortex (practically: 3 cm above the inion). Sometimes two active electrodes are used, one for each hemisphere. The (single) reference electrode is placed at the forehead. For both ERG and VEP, a differential amplifier is used and therefore a ground electrode is needed as well, placed at, for example, an earlobe or (ERG only) the forehead.

Figure 10.1: Electrodes for electrophysiology. Upper row: ERG. Top left: contact lens electrode; top middle: DTL electrode; top right: active electrode below the eye (white), reference electrode at temporal bone (red), ground at forehead (green). Lower row: VEP. Skin electrode (bottom right) and its placement (bottom left).

10.2 Signal and noise

The typical size of an intracellularly recorded signal is 100 mV; the typical size of an ERG signal is 1 mV and of a VEP signal 10 μV. Hence, an accurate recording of these signals is a technical challenge. Sources of noise are (1) the patient him/herself, (2) the electrodes, and (3) interference by the mains ('hum').

Ad 1: The patient must sit still and relax: any muscle activity causes electrical activity in the body as well! Also, in case of VEP, any non-visual brain activity adds noise to the signal (note: for a neurologist this noise is signal: EEG).

Ad 2: Noise originating in the electrodes consists of, amongst others, thermal noise. It can be reduced by taking care of a low electrode impedance (5 kΩ or less at 10-100 Hz) and low-pass filtering. A DTL electrode consists of a silver-coated nylon wire. For a low impedance, a sufficiently deep placement in the fornix is pivotal. For a low impedance skin electrode, the metal electrode must be chloridized (e.g., an Ag/AgCl electrode) and a conducting paste should be used for conductance and stable fixation.

Ad 3: Interference by the mains may result from three mechanisms: *i*. leakage current, *ii*. capacitive coupling, and *iii*. induction. Each medical device is tested for the presence of leakage current before it is allowed to enter the hospital. As such, this source of noise should already

be minimized (typical upper limit: 100 μA). However, it is minimized from the point of view of patient safety; this does not guarantee negligible noise. Capacitive coupling refers to the situation where an electrical wire connected to the mains and the body of the patient together form a capacitor. Capacitive coupling can be reduced by increasing the distance between wire and body or shielding the patient in a Faraday cage. Induction occurs if the wires from the active and reference electrode follow a different route to the amplifier: in this case they form a loop and thus any non-stationary magnetic field (e.g., from the mains) will induce an electromotive force (voltage). Apart from taking away the source of the magnetic field, the straightforward solution is bringing the wires from the two electrodes close to each other, thus reducing the area of the loop.

10.3 Clinical aspects

The primary application of the ERG is assessment of rod and cone function. Rods and/or cones may be absent of malfunctioning congenitally, or may degenerate later. Rod function is assessed with the scotopic (low luminance or dark-adapted) ERG; cone function with the photopic (light-adapted) ERG. In both situations, the entire retina is stimulated uniformly ('Ganzfeld'; Figure 10.2, left panel), with dilated pupil (using mydriatic eye drops). White-light flashes of 5 ms or less are used. The dark-adapted ERG is recorded with flashes of 0.01 cd·s·m^{-2} at a dark background, after 20 min of dark adaptation; the light-adapted ERG with flashes of 3 cd·s·m^{-2} at a background of 30 cd·m^{-2}, after 10 min of light adaptation. If averaging is needed (a single response may be used as well), there should be at least 2 s between the flashes for the dark-adapted ERG and 0.5 s for the light-adapted ERG. The dark-adapted and light-adapted ERG are the two most important of five stimulus conditions prescribed by the International Society for Clinical Electrophysiology of Vision (ISCEV). The ERG can be recorded for both eyes simultaneously.

Figure 10.2: Stimuli for electrophysiology. Ganzfeld stimulus for ERG (left) and checkerboard stimulus for VEP (right).

The primary application of the VEP is assessment of the optic nerve. In most cases of optic neuropathy, the VEP response shows a reduced amplitude; in optic neuritis, the response is

delayed. The primary stimulus is a checkerboard displayed on a monitor (Figure 10.2, right panel); the black squares should be close to 0 cd·m^{-2} and the white squares 100 cd·m^{-2} (i.e., mean luminance is 50 cd·m^{-2} and Michelson contrast 100%). Two square sizes are used: 1° and 0.25°. Black and white checks change phase abruptly (i.e., black to white and white to black) twice per second, that is, at 1 Hz. For a typical VEP, noise exceeds the signal, and averaging over typically 100 reversals is needed. No mydriatic drops should be used; the eyes are stimulated one by one.

Photoreceptors cannot be assessed with a checkerboard stimulus (why not?). If an ERG is recorded while fixating at a checkerboard, a very small response ($\sim$ 10 μV) can be observed, called pattern ERG (PERG), coming from the retinal ganglion cells. Optimal stimulus parameters are check size 0.8°, mean luminance above 80 cd·m^{-2}, Michelson contrast 100%, and 4 (transient PERG) and 16 (steady-state PERG) reversals per second (2 and 8 Hz). Averaging over at least 100 reversals is mandatory. PERG is only used is specialized hospitals or for research purposes. Because many factors influence signal strength in clinical electrophysiology, each lab should determine their own normative values for ERG, VEP, and PERG. Figure 10.3 shows examples of the various responses.

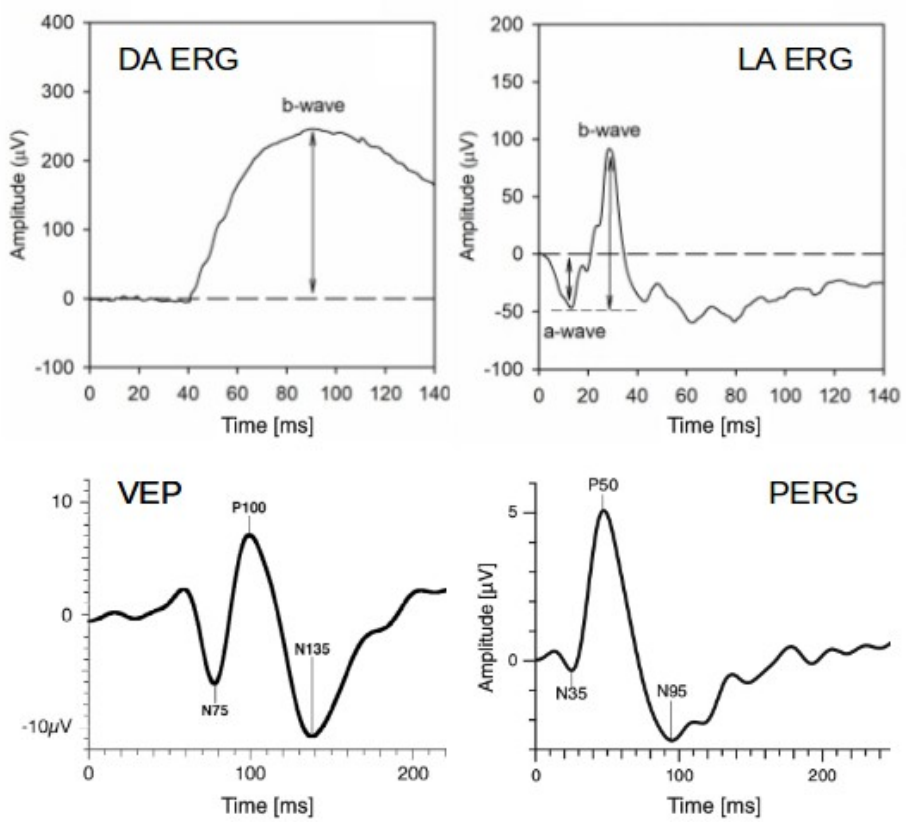

Figure 10.3: Dark-adapted (DA) and light-adapted (LA) ERG, VEP [15], and PERG [1] responses in a healthy subject. ERG a-wave and b-wave originate in the photoreceptor cells and bipolar cells, respectively.

Exercises

1. With reference to Figure 10.3, mention three differences between the dark-adapted and light-adapted ERG response. What is the most obvious difference between the VEP and PERG response? Could you explain this difference?

2. The integration time of the visual system is approximately 100 ms. For stimuli shorter than the integration time, the stimulus is fully characterized by the luminance integrated over time. Calculated the luminance of a dark-adapted ERG stimulus with a duration of (i) 1 ms and (ii) 5 ms.

3. Measured electrophysiology signals are sampled by an analog-to-digital (AD) converter and further processed and analyzed with a computer. Before being sampled, the signals have to be amplified in order to use the resolution of the AD converter in an optimal way, that is, to use the entire voltage range. If the input range of the AD converter ranges from -5 to +5 V, what would be an appropriate amplification factor for ERG? And for VEP?

4. Before being sampled by the AD converter, the signals are not only amplified but also low-pass filtered. What type of noise can be reduced by low-pass filtering? In order not to loose relevant components of the signal, the cut-off frequency of the low-pass filter is recommended to be at least 300 Hz for ERG and 100 Hz for VEP. What sample rate should be used for the AD converter?

5. Electrodes consist of a metal and a corresponding salt. They convert ion current in tissue and conducting paste to electron current in metal. This results in a DC offset due to the half-cell potential. For an Ag/AgCl electrode, the half-cell potential is approximately 0.2 V, which is large compared to the ERG and VEP signal size. Theoretically, the DC offset should be annihilated by the mirror half-cell potential in the other electrode and the use of a differential amplifier - if both electrodes are identical and identically connected. But, practically, a residual offset and drift (due to instability of the offset) remains. What (simple) technical solution could be used to get rid of the residual offset and drift?

6. Noise from the mains ('hum') cannot be removed by high-pass or low-pass filtering. Why not? To remove hum that could not be reduced sufficiently by taking away the sources of the hum, a researcher decides to average a series of three ERG responses (rather than using a single response). What is, for the dark-adapted ERG, the optimal inter-flash interval?

A. 2000 ms
B. 2007 ms
C. 2010 ms
D. 2020 ms

Acknowledgement

I would like to thank D.G. Stavenga for critically reading this reader and pointing me to errors and incomprehensibilities. All remaining errors are mine.

Bibliography

[1] Bach M, Brigell MG, Hawlina M, Holder GE, Johnson MA, McCulloch DL, Meigen T, Viswanathan S. ISCEV standard for clinical pattern electroretinography (PERG): 2012 update. Documenta Ophthalmologica. 2013;126(1):1-7.

[2] Campbell FW, Gubisch RW. Optical quality of the human eye. The Journal of physiology. 1966;186(3):558-78.

[3] Dekking HM, Coster HD. Dynamic tonometry. Ophthalmologica. Journal international d'ophtalmologie. International journal of ophthalmology. Zeitschrift fur Augenheilkunde. 1967;154(1):59-74.

[4] Fercher AF. Optical coherence tomography. Journal of Biomedical Optics. 1996;1(2):157-73.

[5] Fercher AF, Drexler W, Hitzenberger CK, Lasser T. Optical coherence tomography-principles and applications. Reports on progress in physics. 2003;66(2):239.

[6] Forbes M, Pico G, Grolman B. A noncontact applanation tonometer: description and clinical evaluation. Archives of ophthalmology. 1974;91(2):134-40.

[7] Fotios S, Goodman T. Proposed UK guidance for lighting in residential roads. Lighting Research and Technology. 2012;44:69-83.

[8] Gramatikov B. Modern technologies for retinal scanning and imaging: an introduction for the biomedical engineer. Biomedical engineering online. 2014;13.52.10.1186/1475-925X-13-52.

[9] Hitzenberger CK. Optical measurement of the axial eye length by laser Doppler interferometry. Investigative ophthalmology & visual science. 1991;32(3):616-24.

[10] Huang D, Swanson EA, Lin CP, Schuman JS, Stinson WG, Chang W, Hee MR, Flotte T, Gregory K, Puliafito CA, Fujimoto JG. Optical coherence tomography. Science. 1991;254(5035):1178-81.

[11] Jansonius NM, Cervantes J, Reddikumar M, Cense B. Influence of coherence length, signal-to-noise ratio, log transform, and low-pass filtering on layer thickness assessment with OCT in the retina. Biomedical optics express. 2016;7(11):4490-500.

[12] Michelson AA, Morley EW. On the Relative Motion of the Earth and of the Luminiferous Ether. Sidereal Messenger. 1887;6:306-10.

[13] Nio YK, Jansonius NM, Fidler V, Geraghty E, Norrby S, Kooijman AC. Age-related changes of defocus-specific contrast sensitivity in healthy subjects. Ophthalmic and Physiological Optics. 2000;20(4):323-34.

[14] Norren D van. Kleurzienstoornissen. Collegediktaat, University of Utrecht. 1986.

[15] Odom JV, Bach M, Brigell M, Holder GE, McCulloch DL, Tormene AP. ISCEV standard for clinical visual evoked potentials (2009 update). Documenta ophthalmologica. 2010;120(1):111-9.

[16] Schmitt JM. Optical coherence tomography (OCT): a review. IEEE Journal of selected topics in quantum electronics. 1999;5(4):1205-15.

[17] Shlaer S. The relation between visual acuity and illumination. The Journal of general physiology. 1937;21(2):165-88.

[18] Stockman A, Sharpe LT. Into the twilight zone: the complexities of mesopic vision and luminous efficiency. Ophthalmic and physiological optics. 2006;26(3):225-39.

[19] Westheimer G. Scaling of visual acuity measurements. Archives of Ophthalmology. 1979;97(2):327-30.

[20] Wojtkowski M. High-speed optical coherence tomography: basics and applications. Applied optics. 2010;49(16):D30-61.

[21] Yaqoob Z, Wu J, Yang C. Spectral domain optical coherence tomography: a better OCT imaging strategy. Biotechniques. 2005;39(6):S6-13.